Semisynthetic Approach toward Biologically Active Derivatives of Phenylspirodrimanes from *S. chartarum*

Katharina Steinert, Nina Berg, Dmitrii V. Kalinin, Annika Jagels, Ernst-Ulrich Würthwein, Hans-Ulrich Humpf, and Svetlana Kalinina*

Read Online

ACCESS | 📊 Metrics & More | 📖 Article Recommendations | 🆂🅸 Supporting Information

ABSTRACT: The phenylspirodrimanes (PSDs) from *Stachybotrys chartarum* represent a structurally diverse group of meroterpenoids, which, on the one hand, exhibit a structural exclusivity since their occurrence is not known for any other species and, on the other hand, offer access to chemically and biologically active compounds. In this study, phenylspirodrimanes **1−3** were isolated from *S. chartarum* and their water-mediated Cannizzaro-type transformation was investigated using quantum chemical DFT calculations substantiated by LC-MS and NMR experiments. Considering the inhibitory activity of PSDs against proteolytic enzymes and their modulatory effect on plasminogen, PSDs **1−3** were used as a starting material for the synthesis of their corresponding biologically active lactams. To access the library of the PSD derivatives

and screen them against physiologically relevant serine proteases, a microscale semisynthetic approach was developed. This allowed us to generate the library of 35 lactams, some of which showed the inhibitory activity against physiologically relevant serine proteases such as thrombin, FXIIa, FXa, and trypsin. Among them, the agmatine-derived lactam **16** showed the highest inhibitory activity against plasma coagulation factors and demonstrated the anticoagulant activity in two plasma coagulation tests. The semisynthetic lactams were significantly less toxic compared to their parental natural PSDs.
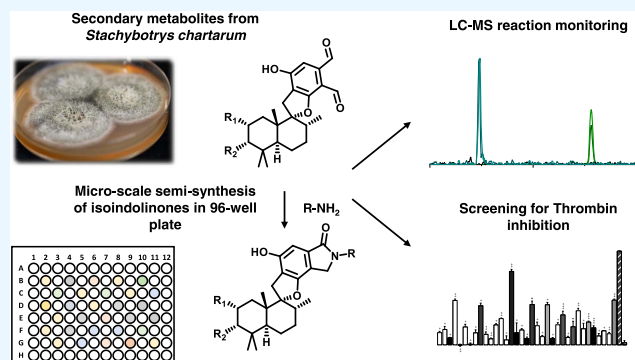
INTRODUCTION

Stachybotrys chartarum is a fungus of the genus *Stachybotrys* whose occurrence is described in dead plant materials and buildings affected by water.[1,2] Due to its secondary metabolites, long-term exposure to *S. chartarum* may pose adverse health effects to humans.[3,4] Two primary chemotypes have been described for *S. chartarum*, which are characterized and distinguished by the production of certain secondary metabolites. While the group of macrocyclic trichothecenes (MCTs, e.g., satratoxins) are only found in strains of chemotype S, atranones are only produced by strains of chemotype A.[5,6] Phenylspirodrimanes (PSDs) are produced by both chemotypes of *S. chartarum* and account for the most abundant group of metabolites produced by all known *Stachybotrys* species.[7−9]

Phenylspirodrimanes (e.g., **1−3**) are triprenyl phenols whose biosynthetic precursor LL-Z1272β (**4**, also known as ilicicolin B) is a well-known key intermediate in the biosynthesis of several meroterpenoid structures.[10,11] **4** originates from orsellinic acid (**5**) and farnesyl diphosphate (**6**, FPP) and is, therefore, a product of the mevalonate and the polyketide pathways (Figure 1).[10,12] Several mechanisms for the biosynthetic rearrangement of **4** to the phenylspirodrimanes are suggested, which include cyclization reactions and

an electrophilic addition leading to the spirofuran ring, which is the linkage between the drimane backbone and the aryl part.[13,14] Some known PSD representatives carry highly reactive *o*-dialdehyde groups at their aryl fragment. These PSDs include stachybotrydial (**1**), stachybotrydial acetate (**2**), and acetoxystachybotrydial acetate (**3**). Structurally, these compounds are unique and only known to be produced by *Stachybotrys* genera.[14] Another group of *Stachybotrys'* metabolites originating from **4** belongs to stachybotrychromenes (e.g., **7**; Figure 1), which are formed *via* the epoxidation of different double bonds of the farnesyl group and therefore are products of a different mode of cyclization.[11,15−17] Stachybotrychromenes from several strains of the genus *Stachybotrys* and *Stachybotrys microspora* triprenyl phenols (SMTPs) exhibit similar structures carrying highly reactive dialdehyde groups on their benzodihydropyran (chroman) moiety. Instead of a
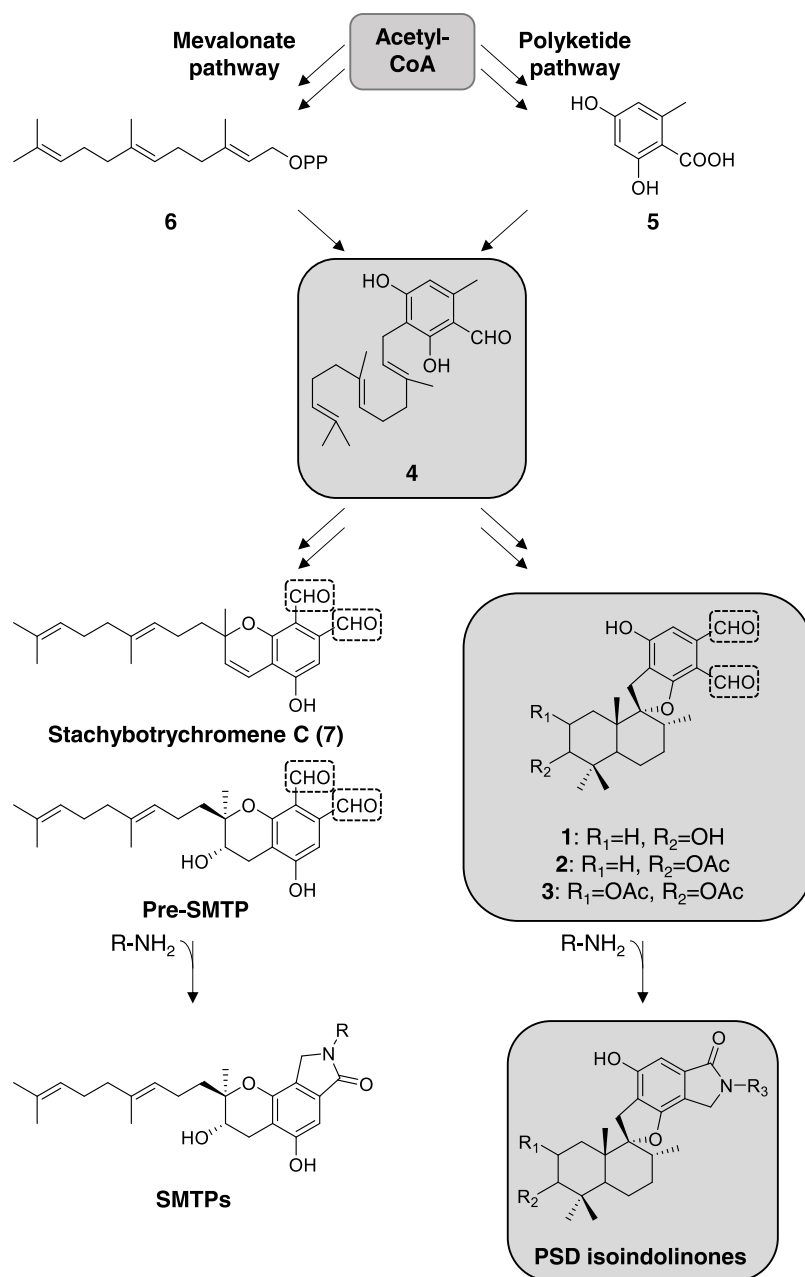
Figure 1. Putative biosynthetic pathway of PSDs and SMTPs. Both groups of compounds are derived from **4** (LL-Z1272β or ilicicolin B) and are formed by different cyclization reactions. For both groups of meroterpenoids, *o*-dialdehydes are known to react with primary amines giving isoindolinones.

drimane skeleton, the farnesyl moiety is present here in an open-chain form.[11,15]

All *o*-dialdehydes from *Stachybotrys* are highly reactive species susceptible to a nucleophilic attack by different nucleophiles. Thus, structurally different derivatives of this kind are known to react with water and amines to form isobenzofuranones (lactones) and isoindolinones (lactams), respectively.[16,18] For the group of SMTPs, the reaction with primary amines was successfully utilized to generate a series of lactams exhibiting targeted activity as plasminogen modulators.[19,20]

Considering the high reactivity of the phthalic aldehydes, it is likely that the described isoindolinones arose from the nonenzymatic reactions with ammonium ions or particular medium components rather than from the secondary metabolism of the fungus. The reaction with ammonium appears to be a spontaneous reaction in which the dialdehydes capture free ammonium.[16] This explains the different isoindolinone contents in N-rich and N-poor media.[5] In addition, lactam-based structures were considered as possible artifacts in the isolation process by Jarvis.[21]

Besides their structural diversity, phenylspirodrimanes also represent versatility in terms of bioactivity. For example, for K-76, a substance related to stachybotrydial (**1**), the inhibitory activity toward the complement system is described.[22,23] Besides this, antiviral and *Glu*-plasminogen-modulating activities for phenylspirodrimanes are described. Here, the compounds tested in the form of dialdehydes showed a higher activity compared to those in lactone or lactam forms.[24,25] Some phenylspirodrimanes are also known for their inhibitory
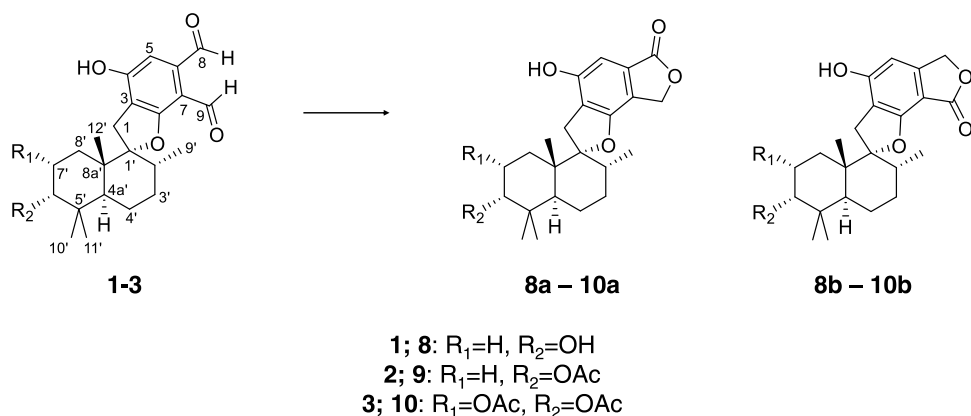
Figure 2. Isomerization of PSDs **1–3** to phthalides **8a–10a, 8b–10b**.

1; 8: R$_1$=H, R$_2$=OH
2; 9: R$_1$=H, R$_2$=OAc
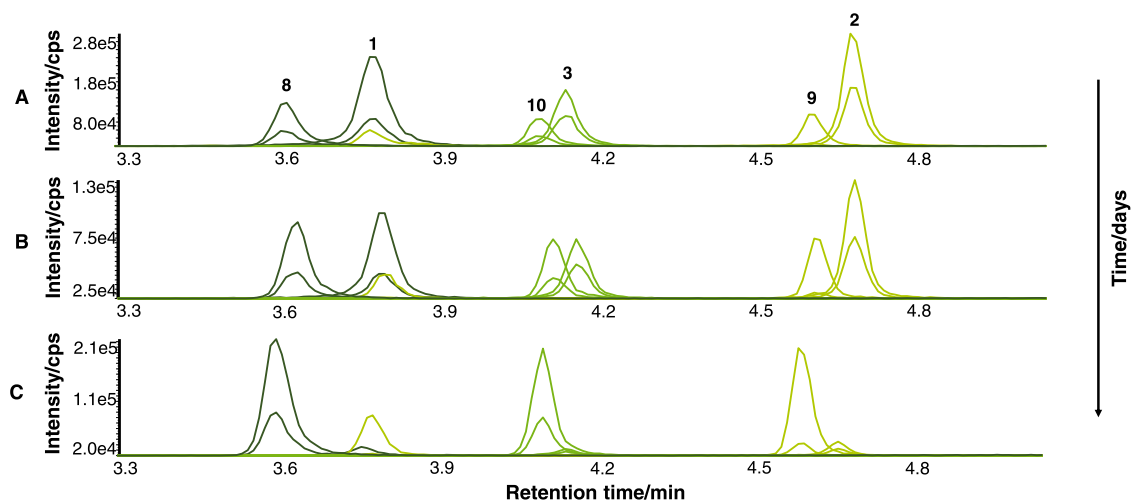**3; 10**: R$_1$=OAc, R$_2$=OAc

Figure 3. LC-MS/MS chromatograms (XIC, SRM mode, negative ionization) of the conversion of *o*-dialdehyde derivatives **1–3** to the corresponding phthalides **8–10a,b** after 2 days (A), 5 days (B), and 30 days (C) of storing in MeCN/H$_2$O + 0.1% FA at −20 °C in the dark.
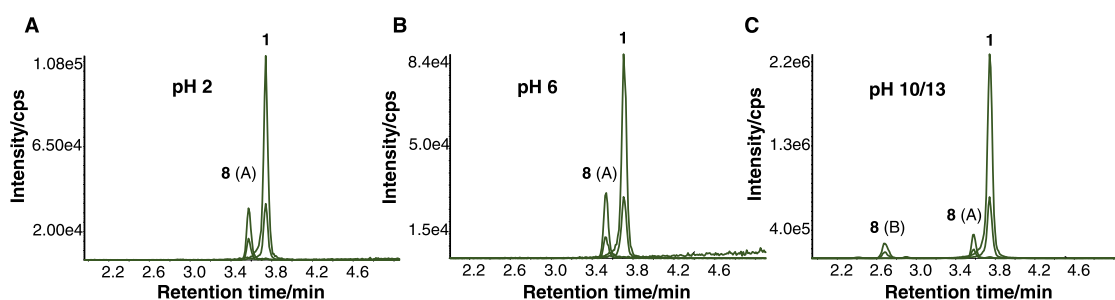

Figure 4. LC-MS/MS chromatograms (XIC, SRM mode, negative ionization) of **1** at 20 °C, pH values 2 (A), 6 (B), and 10/13 (C).

activity against HIV-1 proteases as well as avian myeloblastosis virus (AMV) proteases.[26,27]

Considering that in previous studies lactams of PSDs efficiently inhibited proteolytic enzymes and were also found to be modulators of plasminogen, it is interesting to get access to a series of lactams of PSDs and test them against structurally and functionally related serine proteases of the blood coagulation cascade. Such inhibitors may serve as prospective antithrombotic drugs. It is also encouraging that structurally related natural products have potentially low toxicity,[28] which may further enable their application as therapeutic agents. It is, therefore, also interesting to assess the potential toxicity of produced lactams of PSDs. In this article, we report the

isolation of PSDs from *S. chartarum*, which were then used as a starting material for the microscale parallel synthesis of PSDs' lactams. These new semisynthetic products were investigated for their cytotoxicity profile and found to be active inhibitors of selected serine proteases of the blood coagulation cascade.

## ■ RESULTS AND DISCUSSION

Isolation of Phenylspirodrimanes. To isolate PSDs (**1–3**), a large-scale cultivation of *S. chartarum* IBT 40288 was performed (see the Experimental Section). The extract of *S. chartarum* was fractionated by silica gel column chromatography, followed by semipreparative LC-UV to yield 12.7 mg of **1**, 7.2 mg of **2**, and 27.1 mg of **3**. Isolated compounds were

Thermodynamic Cyclization
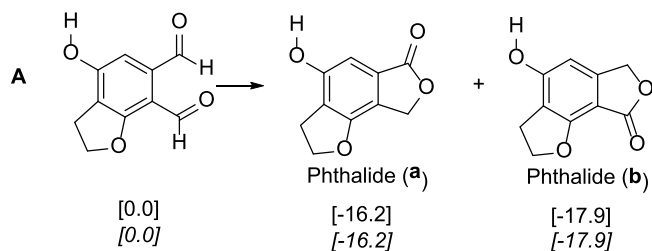
Dihydrate - Hydride Transfer
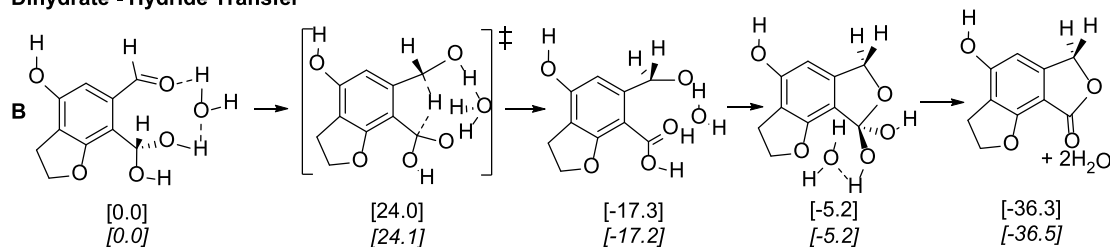
Dihydrate - Anion - Hydride Transfer

TPSSTPSS/def2tzvp + GD3BJ + PCM-MeCN ΔG(298)/kcal/mol
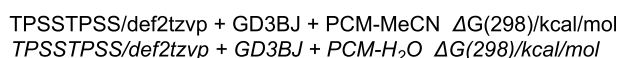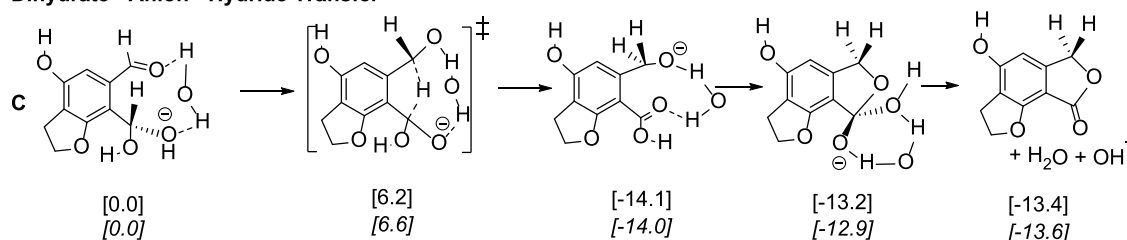*TPSSTPSS/def2tzvp + GD3BJ + PCM-H₂O ΔG(298)/kcal/mol*

Figure 5. Quantum chemically determined thermodynamics of the intramolecular Cannizzaro transformation (based on simplified dialdehyde) (line A); calculated reaction energies using a dihydrate model with hydride migration as transition state (line B) and of the respective monodeprotonated dihydrate model (line C). ΔG_{298} in [kcal/mol], DFT-method used: TPSS/TPSS/DEF2TZVP + GD3BJ + PCM (MeCN) and PCM (H$_2$O) (complete optimization of several conformers (reaction path calculations for transition states) and subsequent frequency calculations to characterize the stationary points and for the determination of ΔG(298 K)).

characterized by high-resolution mass spectrometry (HRMS) and NMR (see the Experimental Section).

Isomerization of Phenylspirodrimanes/Formation of Phthalides. Isolated PSDs (**1−3**) being *o*-dialdehydes might be isomerized into phthalides **8−10a,b** (Figure 2).

The mechanism of this type of isomerization is based on an intramolecular Cannizzaro reaction, which requires basic conditions.[29,30] Interestingly, during the storage of PSDs in slightly acidic aqueous solutions (MeCN/H$_2$O with 0.1% FA, pH value 5−6), we observed the formation of phthalides. However, only one of the two possible phthalide forms was detected, which chromatographically eluted in proximity to the respective dialdehyde (Figure 3).
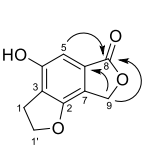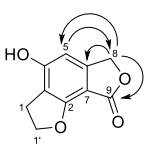
To investigate the formation of a second phthalide form, several experiments with various pH values were performed. LC-MS/MS chromatograms of **1** were recorded at pH values of 2, 6, 10, and 13 (Figure 4), and the peak area ratio of **1**/**8** was determined. At pH values of 2 and 6, similar ratios between **1** and **8a** were observed (factors 4.4 and 3.7). Interestingly, it was found that at pH values of 10 and 13, a second phthalide peak occurred, eluting about one minute earlier (Figure 4c) but exhibiting the same characteristic SRM transitions. The two forms of phthalides were found to have roughly the same ratio from one to another, with the ratio of **1**/**8** (both phthalide forms) being somewhat higher (factor

5.9). This means that phthalide formation takes place to less extent at these pH values.

Quantum Chemical Density Functional Theory (DFT) Calculations. *Assignment of NMR Signals.* To clarify and confirm the second phthalide formation in an alkaline environment, sodium hydroxide solution was added to **3** resulting in the formation of **10** (phthalide **b**), which was then isolated. The structures of **10a** and **10b** were identified by comparing DFT−NMR data (TPSS/def2tzvp+GD3BJ+PCM-(MeCN))[31−36] of simplified model compounds phthalide (**a**) and phthalide (**b**) with experimental NMR data of **10a** and **10b**, as well as by HMBC correlations. Based on these data, the structures of both phthalide variants (**a** and **b**) could be confirmed. Simplified structures as shown in Figure 5 were used for respective quantum chemical calculations (Table 1).

Mechanism of the Intramolecular Cannizzaro-Type Transformation. The presence of water has a decisive influence on the formation of the phthalides because when stored in aprotic solvents, the dialdehyde derivatives proved to be stable for a longer period. Experiments with isotope-labeled H$_2$¹⁸O proved that water is only involved in an intermolecular manner and confirmed the literature on the Cannizzaro reaction.[37] In good agreement with the experimental results, density functional theory (DFT) calculations showed that phthalide (**a**) is the thermodynamically less favorable product

Table 1. Quantum Chemically Calculated (calc., PCM MeCN) and Experimentally (exp., MeCN-d_3-Solutions) Determined ^{1}H and ^{13}C NMR Data of the Two Possible Phthalide Forms as Experimentally Obtained from o-Dialdehyde Derivatives[a]

phthalide (a)   phthalide (b)

C-No.	δ$_C$		δ$_H$ (J in Hz)		δ$_C$		δ$_H$ (J in Hz)	
	calc. (a)	exp. (10a)	calc. (a)	exp. (10a)	calc. (b)	exp. (10b)	calc. (b)	exp. (10b)
1	31.6	32.5	3.19; 3.21	3.07 (dd), (16.8, 17.5)	30.4	31.6	3.12; 3.13	2.98 (dd), (15.9, 16.6)
2	158.7	155.2			162.5	159.8		
3	121.0	120.6			114.6	114.5		
4	157.7	156.3			161.3	160.7		
5	101.6	103.3	6.56	6.73	100.2	101.6	6.17	6.42
6	128.2	128.5			153.3	151.3		
7	122.0	119.9			101.8	101.0		
8	175.0	171.7			74.6	69.0	5.06; 5.06 (13.1)	5.15
9	72.8	68.1	5.10 (d); 5.09 (d), (12.5)	5.17	172.3	169.0		
1'	79.8	99.7			80.6	100.7		

[a]The calculated δ values (in ppm) are for a simplified model of the phthalides.

with a free enthalpy ΔG_{298} of −16.24 kcal/mol in contrast to −17.87 kcal/mol of phthalide (**b**) (Figure 5, line A). Consequently, it is concluded that the reaction is guided mainly by kinetic causes, considering the higher electrophilicity and steric accessibility of C-8 in comparison with that of C-9. The PCM (polarizable continuum model)-acetonitrile solvent model was employed for these calculations throughout; however, relative energies obtained using the PCM−water model for neutral species differ only slightly from the MeCN values (<1 kcal/mol; see Figure 5). As a starting point for the reaction mechanism, a dihydrate model can be assumed undergoing a hydride migration leading to a carboxylic acid/ alcohol intermediate; then, an ester hydrate is formed, which is finally converted into the lactone observed (Figure 5, line B). However, a model involving the dialdehyde, one water molecule, and a hydroxide anion (Figure 5, line C) gives a substantially lower activation energy due to the negative total charge. The latter mechanistic model is close to the experimental reaction conditions and shows the lowest energy barrier compared to various other investigated models. The dihydrate model by BOWDEN et al. provided the basis for the calculations; they also considered hydride transfer *via* mono- and dianions[30] (see also the Supporting Information).

Derivatization of Phenylspirodrimanes with Arginine. The dialdehyde moiety of phenylspirodrimanes is known to exhibit a high chemical reactivity toward primary amines.[38] It is therefore plausible that the phenylspirodrimanes

from *S. chartarum* could be converted to lactams in a manner reported for SMTPs from *S. microspora*.[20,39] It is especially interesting to test the reactivity of isolated PSDs toward amino acids and amines mimicking amino acid structures. This should allow the generation of peptidomimetics targeting serine proteases of interest. Since arginine derivatives and other compounds containing a guanidino group are known to target the active site of serine proteases causing their inhibition,[40,41] derivatization products containing arginine should be prepared and tested first.

To generate the arginine-derived PSDs, two different approaches were examined. First, the amino acid L-arginine at various concentrations (5, 10, 20 mM) was supplemented to the medium on which *S. chartarum* was cultivated, and the formation of the target compounds was confirmed by the extraction of *S. chartarum* cultures with subsequent LC-UV-HRMS analyses. Although the formation of lactams **11−13** was confirmed, the isolation of individual target compounds was found to be problematic due to their similar chromatographic behavior (coelution of **11−13** was observed; Figure S1, Supporting Information).

As an alternative to supplementing arginine to the medium, we attempted to obtain the target compounds *via* their semisynthesis. For this purpose, isolated phenylspirodrimanes reacted with L-arginine in MeCN/water at room temperature in the dark. These mild conditions were required to prevent possible lactone remodeling, which is described for dialdehydes
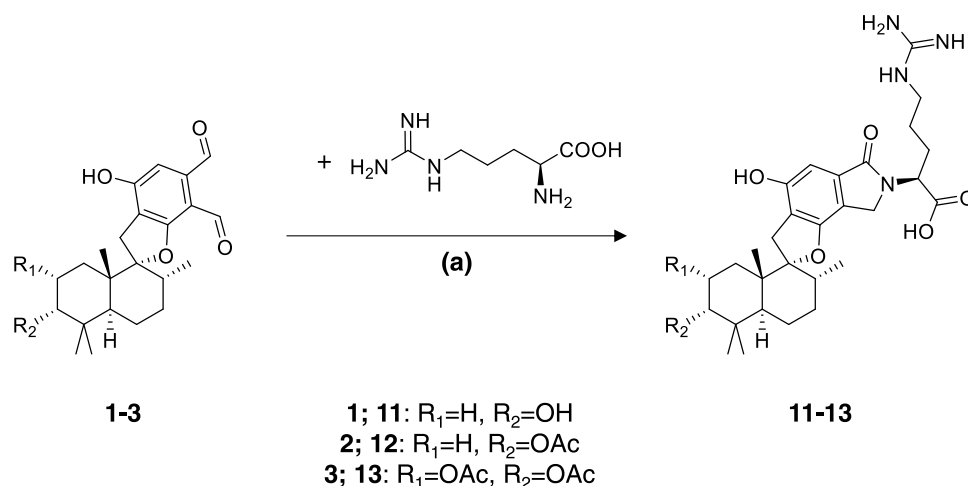
Figure 6. Semisynthesis of lactams **11−13** from phenylspirodrimanes **1−3** and 2 equiv of arginine. (a) MeCN/H$_2$O, r.t., 1−3 h; **11**, 9%; **12**, 14%; and **13**, 13%.
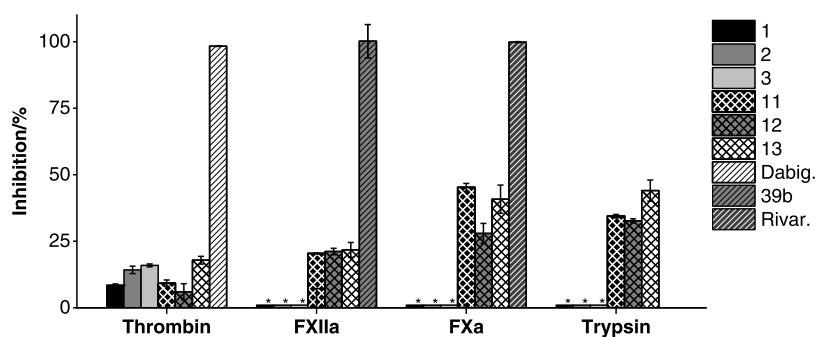

Figure 7. Inhibitory activity of compounds **1−3** and **11−13** toward selected serine proteases. Compounds were tested in triplicate at 200 μM. Dabigatran (Dabig.), rivaroxaban (Rivar.), and compound "**39b**" were used as positive controls at 500 nM for thrombin, FXa, and FXIIa, respectively. * For compounds **1−3**, no inhibition toward FXIIa, FXa, and trypsin was observed.

to occur in protic solvents.[29] Furthermore, the reaction is complicated by the possible formation of dimers and regioisomers. The reaction progress and the successful formation of the target product were monitored at frequent intervals by LC-UV-ELSD and LC-UV-HRMS (Figure S2, Supporting Information). Depending on the phenylspirodrimane derivative used, the reaction was shown to proceed with varying efficiency under different reaction conditions and run times. With the reaction conditions described in Figure 6, the best conversion of the reactants to the target compounds was observed.

Inhibition of Serine Proteases. The isolated PSDs **1−3** and their arginine derivatives **11−13** obtained by semisynthesis were tested *in vitro* for the inhibitory activity against selected serine proteases at a screening dose of 200 μM. The main focus was placed on factors of the blood coagulation cascade such as thrombin, FXa, and FXIIa as these enzymes are known drug targets. Also, tests were performed against another physiologically relevant serine protease trypsin. Tests were performed employing fluorogenic substrates, as reported previously.[42] Whereas PSDs **1−3** showed little (thrombin) to no (FXIIa, FXa, and trypsin) inhibitory activity, their arginine-derived lactams **11−13** inhibited selected serine proteases more potently (Figure 7). Lactams **11−13** inhibited the proteolytic activity of thrombin by 6−18%, FXIIa by 20−22%, FXa by 28−45%, and trypsin by 33−44% at the applied dose. Thus, the derivatization with arginine seemed to have a

significant influence on the inhibitory activity of phenyl-spirodrimanes and even enabled us to achieve minor but significant selectivity among individual enzymes. The inhibitory effects of the phenylspirodrimanes modified with arginine encouraged us to further diversify the structure of PSDs **1−3** to find even more potent inhibitors of blood coagulation-related serine proteases *via* semisynthetic approach.

Microscale Synthesis and Screening. As arginine-derived PSDs **11−13** showed enzyme inhibitory activity in screening tests, it is promising to further modify the structures of PSDs with amino acids and other primary amines to get lactams capable of addressing different pockets in the active site of the targeted serine proteases. The production of lactams, however, is laborious and time-consuming as it requires fungi cultivation on a large scale to isolate sufficient amounts of pure PSDs. Moreover, the purification of semisynthetically obtained final products is also not a trivial task requiring multiple efforts using individual semipreparative LC conditions for each derivative. Therefore, we aimed to develop a method allowing for the fast generation of a library of PSD derivatives from small quantities of the starting materials to permit their subsequent screening against serine proteases.

During the method development, the conventional semi-synthesis was first simplified and transferred to the 96-well plate format allowing the parallel synthesis on microscale. The reactions were performed in lower volumes and higher
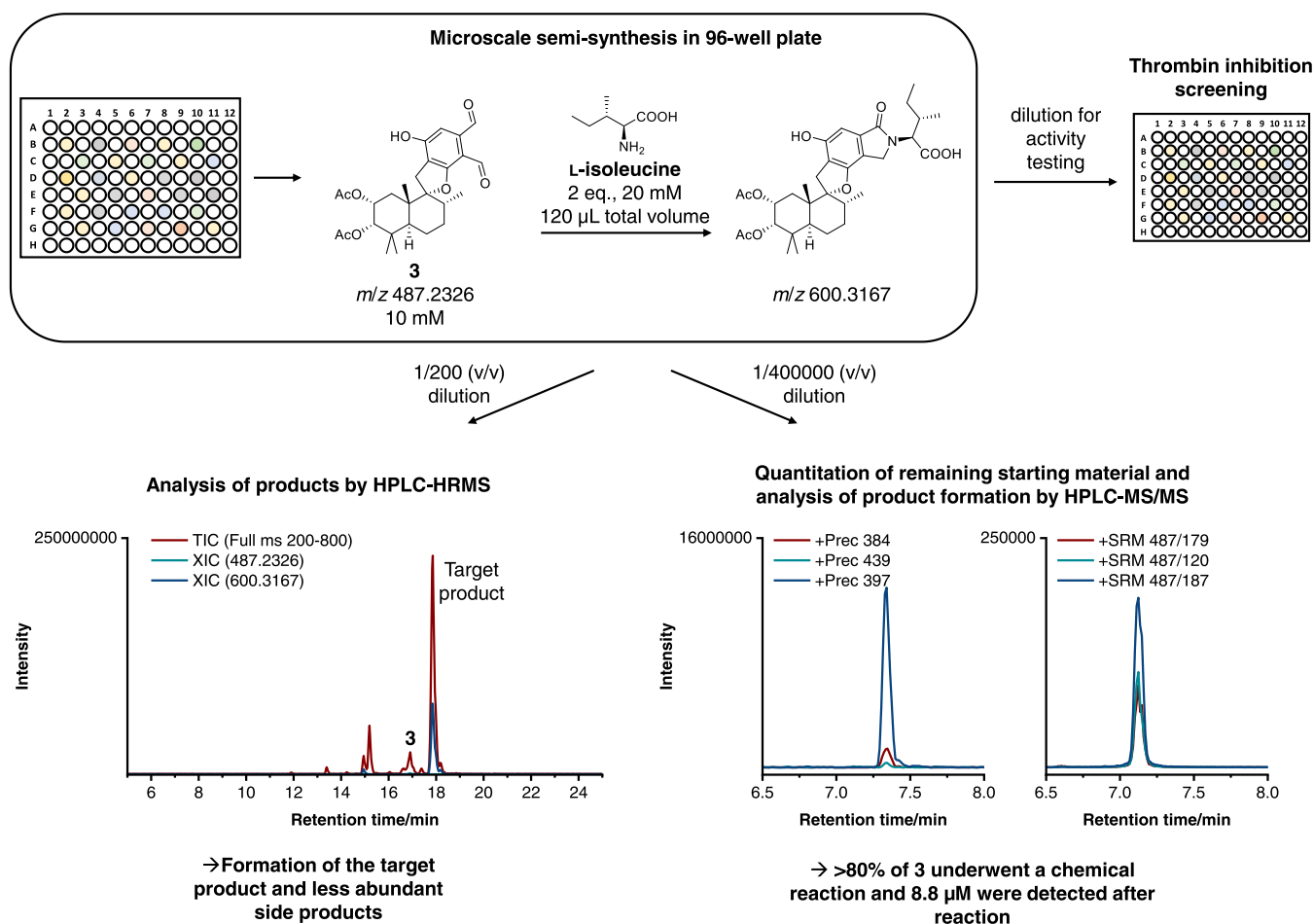
Figure 8. Workflow of the microscale semisyntheses of lactams in a 96-well plate combined with their screening against thrombin. The microscale reaction is exemplarily shown for **3** with L-isoleucine.

concentrations in a total volume of 120 μL of MeCN/H$_2$O at 10 mM of PSD **3**. For the microscale synthesis, PSD **3** was selected as a starting material based on its inhibitory activity and the activity of its arginine derivative **13** (Figure 7). Also, PSD **3** was produced and isolated in the highest amount compared to **1** and **2**. The reaction time was set to 4 h, as it has been shown that in a model microscale reaction between **3** and arginine, the full consumption of **3** was observed after 4 h (Figure S2, Supporting Information). As we planned to use nonisolated final products (lactams) directly from the reaction mixtures for the biological activity screening, it was important to measure the final product concentration at the end of the reaction. This should ensure that all of the compounds are tested at the same final concentration (achieved in the subsequent dilution step). For this, a robust and sensitive quantitative method should be developed. The general workflow of the microscale synthesis and subsequent activity screening is displayed in Figure 8, exemplary for the reaction of **3** with L-isoleucine.

Reaction Monitoring by LC-MS/MS and LC-UV-HRMS. For the microscale reaction monitoring, we utilized LC-MS methods. Nevertheless, selected reaction monitoring with determination of the reaction conversion rate is not a trivial task due to several reasons. First, the quantitation based on external calibration with purified reference standards of the final products is not possible as these products are not available. Second, the mass spectrometric response of the

products is different in each reaction given the structural diversity of the reactants. Therefore, reaction monitoring is only possible based on the quantitation of the starting material remaining in a semiquantitative manner. As the starting material consumption might be related not only to the desired product formation but also due to side reactions, it is also important to monitor the formation of the target compound. Considering the above-mentioned, the following LC-MS/MS method was developed. The isolated reference standard of **3** (starting material, SM) was used to optimize SRM transitions for quantitation of the remaining **3** over a linear concentration range of three decades (0.001−1 μM) (SM). Exemplarily, a LC-MS/MS chromatogram of compound **3** (0.1 μM) is presented in Figure S28, Supporting Information. Based on Mandel's fitting test and the coefficient of determination (R^2 = 0.994), the quantitation of the unreacted **3** was done by linear calibration. The limit of detection (LOD) for **3** was 0.0002 μM, and the limit of quantification (LOQ) was 0.001 μM. To detect the formation of the final reaction product (lactam) in the same measurement, additional precursor ion scans were integrated into the method. The most abundant fragment ions of the isolated reference standard of **13** were used, and the fragmentation parameters were optimized. In addition, the conversion of the reaction was critically examined qualitatively by LC-UV-HRMS.

For the microscale semisynthesis, 35 different primary amines (Table S3, Supporting Information), including various
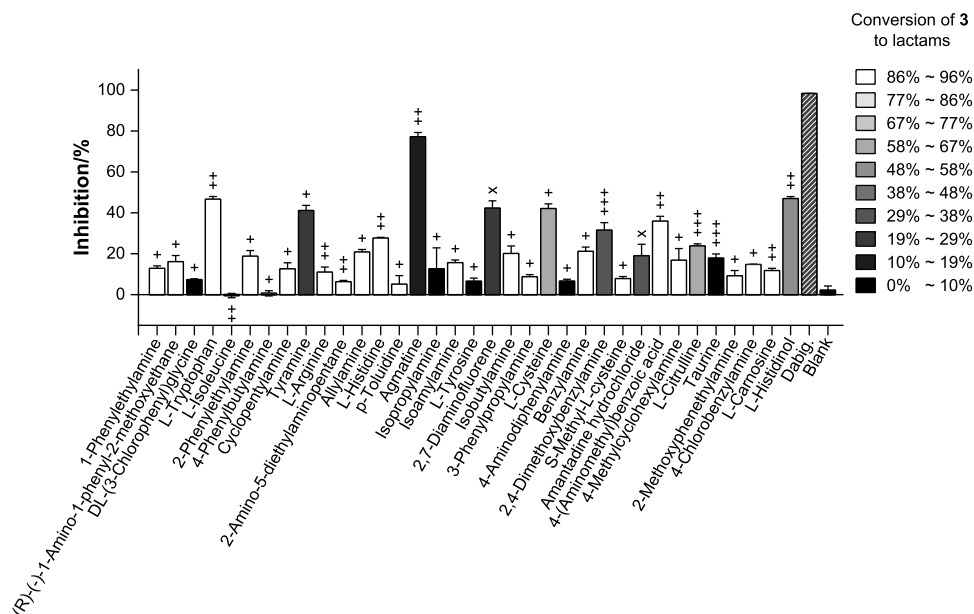
Figure 9. Thrombin inhibition by 36 PSD derivatives obtained by microscale semisynthesis. Tests were performed in triplicate at concentrations of 200 μM of the target compounds, and the average with SD is given. Dabigatran (Dabig., 500 nM) was used as a positive control, and compound **3** treated under reaction conditions without an amine addition was used as a blank sample. In addition, the percent conversion of **3** to reaction products is shown in color intensities. In reactions marked with a +, the target product was formed; in reactions marked with a ++, the target product was formed and it is the most abundant product; in reactions marked with a +++, the target product is the only reaction product and no byproducts were observed; in reactions marked with an x, no product formation was observed. The specific data are given in the Supporting Information in Table S3.
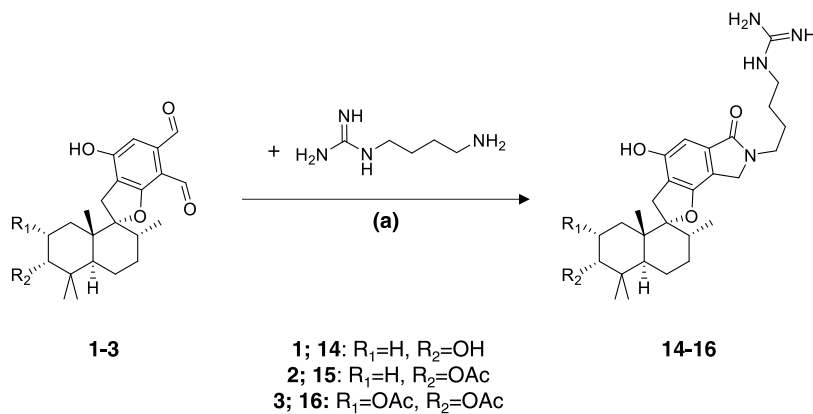

Figure 10. Semisynthesis of lactams **14−16** from phenylspirodrimanes **1−3** and agmatine. (a) MeCN/H$_2$O, r.t., 1−3 h; **14**, 39%; **15**, 22%; and **16**, 33%.

amino acids, reacted with **3** in a 96-well plate. After the reaction completion (4 h), the reaction mixture was taken and diluted stepwise 1/200 (v/v) for LC-HRMS analysis and 1/400,000 (v/v) for LC-MS/MS analysis with MeCN/H$_2$O (10/90, v/v) to determine the reaction conversion. The percent conversion of **3** to the reaction products is shown in color intensities in Figure 9. In general, the majority of lactams were successfully formed, with only a few showing low conversion under applied conditions. No conversion was observed in reactions with isopropylamine, 3-chlorophenylglycine, L-Tyr, taurine, and 4-aminodiphenylamine. Among other amines, natural amino acids such as Trp, Arg, and His as well as *S*-methyl-L-Cys showed close to quantitative conversion into the corresponding lactams.

Screening for Thrombin Inhibitors. The generated library of lactams (microscale reaction mixtures) was screened for thrombin inhibitory activity. Each representative was tested

at the equimolar concentration (200 μM) in a manner analogous to the assays performed for compounds **1−3** and **11−13**. The results of thrombin inhibition are shown in Figure 9 together with the percentage of product (lactams) formation from dialdehyde **3**. It has been found that the formed lactams to a different extent inhibit the targeted enzyme. Among tested compounds, eight lactams significantly inhibited thrombin (30−78%) exceeding the activity of the starting material dial **3**. Other lactams, irrespective of their formation %, showed a lower ability to affect the proteolytic activity of thrombin. The difference in lactams' inhibitory activity was determined by their structure. Thus, lactams derived from Trp, tyramine, agmatine, 2,7-diaminofluorene, Cys, 2,4-dimethoxybenzylamine, 4-(aminomethyl)benzoic acid, and L-histidinol were found to be the most active inhibitors. Some of the formed lactams demonstrated even lower inhibitory activity than **3**. This was especially pronounced for the inactive lactams
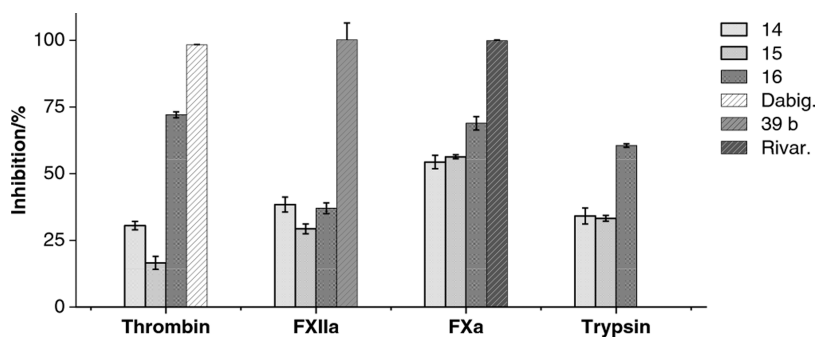
Figure 11. Inhibition of serine proteases by compounds **14−16**. Compounds were screened at 200 μM in fluorogenic-based assays. Tests were performed in triplicate; mean values ± SD are shown. Dabigatran, rivaroxaban, and compound "**39b**" were used as positive controls at 500 nM for thrombin, FXa, and FXIIa, respectively.

derived from Ile and 4-phenylbutylamine (Figure 9). Interestingly, the highest degree of inhibition (77%) was observed upon thrombin incubation with the agmatine-derived lactam. Therefore, agmatine derivative was selected as a lead compound and suggested for further conventional synthesis. This should allow us to test this lactam as an individual pure compound excluding the potential effects of other components of the reaction mixture. Moreover, this should validate the feasibility of the used microscale screening approach for the search for new biologically active compounds.

Semisynthesis and Activity of Agmatine-Derived Phenylspirodrimanes. As the performed screening revealed an agmatine derivative of **3** to be the most active, we conducted semisyntheses of agmatine-based lactams from isolated PSDs **1−3** (Figure 10).

The resulting reaction products **14−16** were purified and tested against thrombin and three other serine proteases at 200 μM (Figure 11). Noticeably, lactam **16** synthesized in a normal scale showed thrombin inhibitory activity (72%) comparable to those found in the screening (77%). Moreover, lactam **16** was found to be an active inhibitor of other tested serine proteases including blood coagulation factors Xa and XIIa as well as trypsin. Although two other synthesized agmatine derivatives **14** and **15** showed inhibition of the tested serine proteases, lactam **16** generally was the most active inhibitor. When considering the structure−activity relationship among these three PSDs, it is apparent that the presence of two acetoxy groups (derivative **16**) is translated into the more pronounced serine protease inhibitory activity, especially toward thrombin. This leads to the assumption that the acetoxy groups on the drimane backbone influence the binding of the compounds to the corresponding binding pockets in the enzymes.

As agmatine-derived lactam **16** showed the ability to inhibit serine proteases of blood coagulation cascade, it might exhibit anticoagulant properties. Therefore, lactam **16** was tested for its anticoagulant activity in two *in vitro* plasma coagulation tests, namely, activated partial thromboplastin time (aPTT) and prothrombin time (PT). These two tests allow us to distinguish whether the extrinsic (PT) or the intrinsic (aPTT) blood coagulation pathway is affected by a test compound. As can be seen from Figure 12, lactam **16** influenced plasma coagulation affecting both aPTT and PT. Thus, when tested at 600 μM, **16** prolonged the plasma coagulation time by 43 and 92% in aPTT and PT tests, respectively. As the plasma coagulation time was extended in both tests, it indicates that compound **16** inhibits blood coagulation factors of both
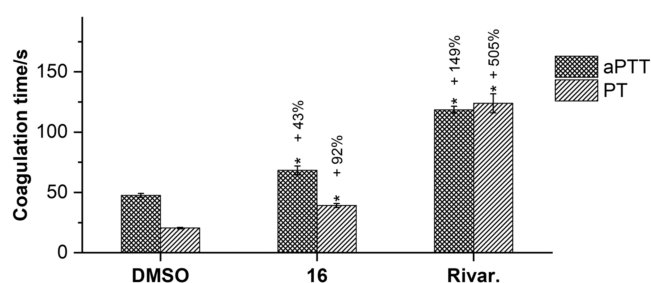

Figure 12. *In vitro* anticoagulant activity (plasma) of **16** tested at 600 μM compared to that of rivaroxaban (Rivar.) tested at 2 μM. The activated partial thromboplastin time (aPTT) and prothrombin time (PT) are shown in seconds. The percentage of aPTT and PT increase compared to the effect of DMSO is shown. Tests were performed at least in triplicate, and the average with SD is given. *statistically significant ($p \leq 0.001$).

aforementioned pathways. This is in agreement with its ability to inhibit thrombin, FXa, and FXIIa (Figure 11). Importantly, the anticoagulant activity of lactam **16** demonstrates that it is active not only *in vitro* on the enzymatic level but also on the macro level in plasma.

Cytotoxicity. Structurally diverse PSDs demonstrate various biological activities including inhibition toward the complement system, *Glu*-plasminogen modulation, and antiviral effects.[22,24] Exposure to *Stachybotrys*, however, is associated with stachybotryotoxicosis and infections of the gastrointestinal and respiratory tract.[3,4,26,43−45] Among others, pulmonary hemorrhage is described as the most common one.[4] Therefore, it is of high importance to estimate the potential cytotoxicity of *Stachybotrys*-derived metabolites. In this study, isolated PSDs (**1−3**) and their semisynthetic analogs **11−16** were tested against human liver cancer cells (HepG2) and adenocarcinomic human alveolar basal epithelial cells (A549). With both cell lines tested, compounds were incubated in a concentration range of 0.1−100 μM. The viability of the cells after 24 h was determined by resazurin reduction assay. In both cell lines, PSDs (**1−3**) demonstrated higher cytotoxic effects in comparison with their semisynthetic analogs (**11−16**) (Figure 13A,B). Thus, the highest cytotoxicity was observed after incubation of the A549 cells with **2** and **3** (for both IC$_{50}$ < 0.1 μM). In contrast, for **11−16**, the cellular viability at the highest tested concentration (100 μM) was >60%. Generally, the A549 cells were found to be more sensitive to all tested compounds (Figure 13A). Concerning toxicity studies on HepG2 cells, the starting materials—PSDs **1−3**—demonstrated a moderate toxicity, of which **3** was found to be the most toxic (Figure
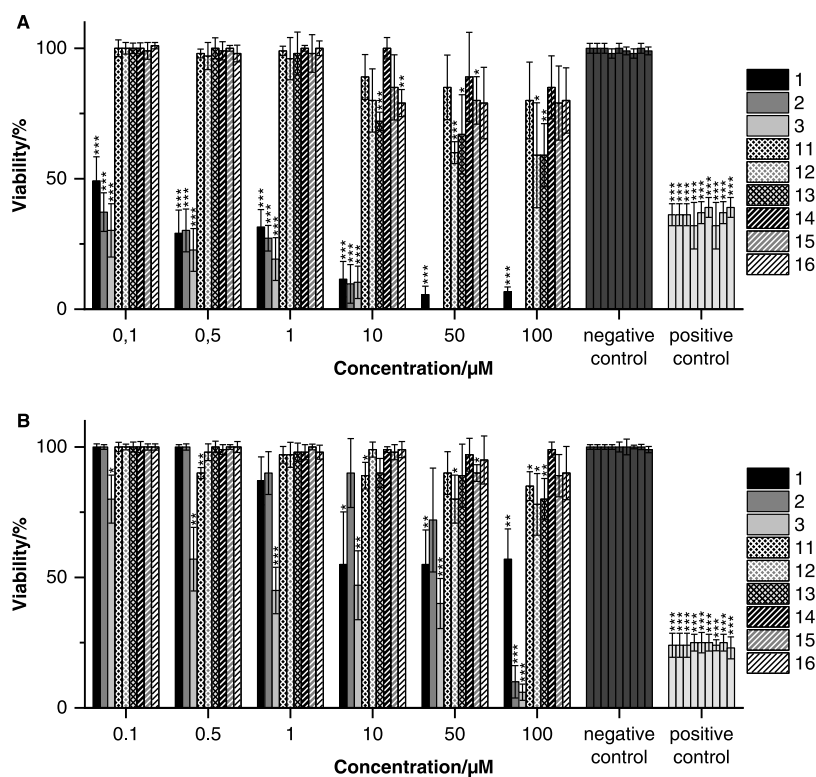
Figure 13. Cytotoxicity of compounds **1–3** and **11–16** tested on A549 (A) and HepG2 (B) cells. T-2 toxin (10 μM) was used as a positive, and DMSO (1%) was used as a negative control. The results represent the sum of three individual experiments, each with three triplicate ($n \geq 9$). *statistically significant $p \leq 0.05$, **$p \leq 0.01$, and ***$p \leq 0.001$.

13B). The cell viability at a concentration of 100 μM for **1** was 57 ± 11.6% and that for **2** and **3** was 10 ± 6.2 and 6 ± 3.1%, respectively (Figure 13B). For semisynthetic derivatives (**11–16**), only slight cytotoxic effects were observed, with HepG2 cell viabilities not lower than 50%.

The results of the cytotoxicity study in both cell lines indicated a significant reduction of the cytotoxicity of PSDs by their derivatization. The dialdehyde functional groups of **1–3** not only offer high reaction potential in chemical terms but also appear to play a remarkable role in cytotoxicity. Nevertheless, based on the results, it can be stated that the less reactive semisynthesis products, for which higher inhibitory activities on serine proteases were observed, exhibited significantly lower cytotoxic effects.

CONCLUSIONS

In conclusion, in this study, phenylspirodrimanes (PSDs) **1–3** exhibiting a dialdehyde moiety were isolated from *S. chartarum* and used as a starting material for the synthesis of their corresponding isoindolinones. Additional efforts were undertaken to investigate the water-mediated intramolecular Cannizzaro-type transformation of **1–3** using theoretical calculations along with LC-MS and NMR experiments. To access the library of the PSD derivatives and screen them against physiologically relevant serine proteases, a microscale semisynthetic approach was developed. A generated library of 35 lactams was tested for the inhibitory activity toward thrombin (FIIa), FXIIa, FXa, and trypsin. Among them, the agmatine-derived lactam **16** showed the highest inhibitory activity. Subsequently, lead compound **16** was shown to demonstrate the anticoagulant properties in two plasma coagulation tests, namely, PT and aPTT. Moreover, it has

been demonstrated that semisynthetic isoindolinones were significantly less toxic compared to their parental natural PSDs. Considering the relatively low cytotoxicity of lactams **14–16** and their serine protease inhibitory profile, these compounds may serve as a starting point for the development of new anticoagulants.

EXPERIMENTAL SECTION

General Experimental Procedures. Full set (^{1}H, ^{13}C, gHMBC, gHSQC, and gCOSY) of NMR spectra was recorded on an Agilent DD2 600 MHz spectrometer (Agilent Technologies, Waldbronn, Germany); chemical shifts (δ) are reported in ppm relative to tetramethylsilane. Thin-layer chromatography was performed on Silica gel 60 F$_{254}$ plates (Merck, Darmstadt, Germany). Purity measurements of the isolated and synthesized compounds were performed on an LC-UV-ELSD with an LC PU-2089 system with UV detection (MD-2010) (Jasco, Groß-Umstadt, Germany) and evaporative light scattering detection (ELSD) (Shimadzu, Duisburg, Germany). A Nucleodur phenyl–hexyl column (250 mm × 4 mm i.d., particle size 5 μm) equipped with a 4 mm × 3 mm i.d. phenyl–hexyl guard column (Macherey-Nagel, Düren, Germany) was used for separation, employing a binary gradient consisting of MeCN and H$_2$O (both containing 0.1% FA). The wavelength of the UV detector was set to 230 nm. The ELSD was set to a temperature of 50 °C, and 350 KPa of pressurized air was used. Purity results are given in the description of the compounds.

High-resolution mass spectrometric data for structural characterization were obtained on an LTQ Orbitrap XL mass spectrometer (Thermo Fisher Scientific, Dreieich, Germany) operated in positive mode and a direct sample injection of a 10

μg/mL solution in MeCN/H$_2$O/FA (50/49.9/0.1, v/v/v) with a syringe pump (5 μL/min). The heater was turned off, the capillary temperature was set to 275 °C, and the sheath gas was set to 5 arbitrary units, with the auxiliary and sweep gases switched off. The spray voltage, capillary voltage, and tube-lens voltage were set to 4 kV, 30 V, and 80 V, respectively. The data were acquired in centroid mode with a resolution of 60,000. MS/HRMS characterization was achieved using the higher-energy collision-induced dissociation (HCD) cell of the orbitrap mass spectrometer by the application of a relatively normalized collision energy individually optimized for each analyte, an activation time of 30 ms, and an isolation width set to 1 m/z. UV maxima were assessed with the LC-UV-HRMS coupling according to the descriptions in the following paragraphs.

All chemicals were purchased in analytical grade from Sigma-Aldrich GmbH (Seelze, Germany), VWR (Darmstadt, Germany), Fisher Scientific (Schwerte, Germany), Grüssing GmbH (Filsum, Germany), or Carl Roth (Karlsruhe, Germany). Purified water was generated using a PURELAB Flex 2 system (Veolia Water Technologies, Celle, Germany). Deuterated NMR solvents were obtained from ARMAR Chemicals (Döttingen, Switzerland).

Fungal Strains and Culture Conditions. Phenylspiro-drimanes (PSDs) were isolated from the *S. chartarum* IBT 40288 strain, obtained from the IBT Culture Collection of Fungi (Technical University of Denmark, Denmark). To obtain precultures, Erlenmeyer flasks with 125 mL of potato broth (20 g/L of dextrose, 4 g/L of potato infusion) were inoculated with approx. 1 cm^2 of agar plugs covered with *S. chartarum* strain. The flasks were cultivated shaken at 180 rpm at 23 °C in the dark for 3 days. Potato dextrose agar (PDA, 20 g/L of dextrose, 15 g/L of agar, 4 g/L of potato infusion) was used for cultivation on a large scale. The agar plates were inoculated with 0.5 mL of *S. chartarum* preculture and cultivated at 23 °C for 3 weeks in the dark. To obtain the arginine derivatives of the PSDs, standard media (PDA) was supplemented with a sterile filtered solution of arginine in various concentrations (5 mM, 10 mM, and 20 mM).

Analysis of the PSDs and their Arginine Derivative Formation in Fungal Cultures. To examine the production of PSDs and their arginine derivatives in *S. chartarum* cultures, a slightly modified method for microscale extraction developed by Smedsgaard was used.[46] Three plugs (approx. 1.0 cm^2) from three independent agar plates were cut from fungal colonies. Each agar plug was transferred to 2 mL of Eppendorf tubes, 1 mL of ethyl acetate (EtOAc) was added, and the samples were vortexed (VF2 Minishaker, IKA Labortechnik, Staufen, Germany) for 30 s. Subsequent extraction was carried out on a laboratory shaker (New Brunswick, Innova 44, Eppendorf, Wesseling-Berzdorf, Germany) for 30 min at 250 rpm. The supernatant was removed, and extraction was repeated two times. The supernatants were combined, transferred into a vial, and evaporated to dryness under a N$_2$ stream at 40 °C. Thereafter, the residue was dissolved in 1 mL of MeCN/H$_2$O (70/30, v/v) and filtered through a 15 mm syringe filter containing a 0.2 μm pore size RC membrane (Phenomenex, Aschaffenburg, Germany). The determination of PSDs and their arginine derivatives was carried out by LC-UV-HRMS (see below).

Isolation of PSDs. For isolation of the PSDs (**1**−**3**), 100 agar plates inoculated with *S. chartarum* strain were cultivated for 3 weeks at 23 °C in the dark. The fungal cultures were

extracted with (2.5 L) of EtOAc on a laboratory shaker (150 rpm). After the medium and mycelium have been removed by filtration through Miracloth (Merck, Darmstadt, Germany), they were extracted again with fresh solvent. The obtained extracts were collected and concentrated *in vacuo* at 40 °C. The residue was dissolved in dichloromethane (DCM) and chromatographically purified on a preparative column using NP silica gel 60 (0.040−0.063 mm, Merck, Darmstadt, Germany). For fractionation, a cyclohexane/EtOAc gradient with ratios (100/0, 90/10, 70/30, 50/50, 30/70, 0/100 (v/v)) was employed. Changes of the solvent mixture and combination of the obtained fractions containing the PSDs were made based on thin-layer chromatography (TLC) analysis. The fractions containing PSDs were further purified with a semipreparative LC-UV Jasco HPLC PU-2087/2087 system and a UV-2075 detector (Jasco, Groß-Umstadt, Germany). The separation was performed on a ZORBAX Eclipse XDB-C18 column (9.4 mm × 250 mm, 5 μm, Agilent, Waldbronn, Germany) equipped with a C18 guard cartridge (4 mm × 3 mm, Phenomenex, Aschaffenburg, Germany) applying a binary gradient consisting of water (solvent **A**) and MeCN (solvent **B**) at a consistent flow rate of 5 mL/min and a 40 °C column oven temperature. The gradient started with 40% **A** for 1 min followed by linearly increasing the percentage of **B** to 100% within 16 min and holding for 2 min. For equilibration, **A** was increased to 40% again for 2 min (chromatogram is shown in Figure S3, Supporting Information).

LC-UV-HRMS Analysis. The LC-UV-HRMS analysis of fractions during isolation progress and monitoring of the microscale semisyntheses were carried out using a Nexera XR LC system (Shimadzu, Duisburg, Germany) coupled with an SPD-M30A diode array detector (Shimadzu, Duisburg, Germany) and an LTQ Orbitrap XL mass spectrometer applying heated-electrospray ionization (HESI) (Thermo Fisher Scientific, Dreieich, Germany) in the positive ionization mode. Chromatographic separation was performed with a binary gradient consisting of MeCN and H$_2$O (both containing 0.1% FA) on a ReproSil Gold C18 column (150 mm × 2 mm, 3 μm, Dr. Maisch, Ammerbuch, Deutschland). The gradient started with 10% MeCN + 0.1% FA (solvent **A**) and 90% H$_2$O + 0.1% FA (solvent **B**) for 2 min and a flow rate of 0.3 mL/min and 40 °C column oven temperature. Within 20 min, **A** was increased linearly to 100%. For the next 5 min, **A** was held at 100%. Equilibration was performed for 5 min with the initial conditions. The source voltage was set to 3.5 kV. Capillary and vaporizer temperatures were set to 350 °C; the sheath gas flow was set to 40 arbitrary units, the auxiliary gas flow was set to 20 arbitrary units, and the sweep gas flow was set to 5 arbitrary units. Full scans were recorded in profile mode with a resolution of 30,000 in a mass range of m/z 100−800. Fragmentation experiments of the respective two most intense ions were performed with higher-energy collisional dissociation (HCD) with a normalized energy of 35%, an activation time of 30 ms, and an isolation width set to 1 m/z. For data acquisition and analysis, the Tune Plus 2.7 and Xcalibur 3.1 software (Thermo Fisher Scientific, Dreieich, Germany) were used.

Semisynthesis of PSDs with Amino Acids. Two equivalents of the amino acid, dissolved in 1 mL of water, were added to 1 equiv of the corresponding PSD, dissolved in 2.5 mL of MeCN. The mixture was stirred for 3 h at room temperature under light exclusion and evaporated under vacuum. For purification of the reaction products, the mixture

was redissolved in 3 mL of MeCN and applied for semipreparative LC-UV on a ZORBAX Eclipse XDB-C18 column (9.4 mm × 250 mm, 5 μm, Agilent, Waldbronn, Germany) equipped with a C18 guard cartridge (4 mm × 3 mm, Phenomenex, Aschaffenburg, Germany) with a MeCN/H$_2$O gradient applying a binary gradient consisting of water (solvent **A**) and MeCN (solvent **B**) at a consistent flow rate of 5 mL/min and a 40 °C column oven temperature. For purification of agmatine derivatives, both eluents contained additionally 0.1% of FA. The gradient programs are shown in the Supporting Information in Table S2. The fractions containing the products were combined and evaporated under vacuum. All semisynthesized compounds were structurally characterized according to the descriptions above.

Stachybotry-arginine (11). Pale yellow powder (4.64 mg, 9%), TLC: 0.26 (DCM/MeOH = 30/70). UV λ$_{max}$ (MeCN/H$_2$O): 224, 268, 304 nm. ^{1}H NMR (600 MHz, MeOH-d_4) δ 0.73 (d, *J* = 6.6 Hz, 3H, H-9′), 0.88 (s, 3H, H-10′),0.97 (s, 3H, H-11′), 1.05 (s, 3H, H-12′),1.07 (m, 2H, H-8′), 1.52 (m, 2H, H-7′), 1.55 (overlapped, 2H, H-4‴), 1.55 (overlapped, 2H, H-4″), 1.59 (m, 2H, H-3′), 1.88 (m, 1H, H-2′), 2,13 (m, 1H, H-4a′), 2.15 (m, 2H, H-3″), 2.84 (d, *J* = 16,7 Hz, 1H, H-1), 3.22 (m, 1H, H-1), 3.24 (m, 2H, H-5‴), 3.33 (m, 1H, H-6″), 4.28 (d, *J* = 17.2 Hz, 1H, H-9), 4.72 (d, *J* = 17.2 Hz, 1H, H-9), 4.75 (m, 1H, H-2″), 6.67 (s, 1H, H-5). ^{13}C NMR (150 MHz, MeOH-d_4) δ 16.0 (CH$_3$, C-9′), 16.6 (CH$_3$, C-12′), 22.1 (CH$_2$, C-4′), 23.0 (CH$_3$, C-10′), 25.3 (CH$_2$, C-8′), 26.1 (CH$_2$, C-7′), 27.2 (CH$_2$, C-4″), 28.8 (CH$_2$, C-3″), 29.0 (CH$_3$, C-11′), 32.3 (CH$_2$, C-3′), 33.0 (CH$_2$, C-1), 38.4 (CH, C-2′), 38.6 (C, C-5′), 41.3 (CH, C-4a′), 41.9 (CH$_2$, C-5″), 43.5 (C, C-8a′), 45.9 (CH$_2$, C-9), 57.7 (CH, C-2″), 76.3 (CH, C-6′), 99.7 (C, C-1′), 102.1 (CH, C-5), 114.9 (C, C-7), 118.7 (C, C-3), 135.1 (C, C-6), 155.1 (C, C-4), 157.6 (C, C-2), 158.6 (C, C-6″), 171.7 (C, C-8), 177.4 (C, C-1″). HRMS (10 μg/mL): *m/z* 543.3166 (calcd for [C$_{29}$H$_{43}$N$_4$O$_6$]$^+$ 543.3177, Δ*m*: −1.2 ppm), purity > 99%.

Stachybotryacetate-arginine (12). Pale yellow powder (2.46 mg, 14%), TLC: 0.33 (DCM/MeOH = 30/70). UV λ$_{max}$ (MeCN/H$_2$O): 224, 268, 304 nm. ^{1}H NMR (600 MHz, MeOH-d_4) δ 0.77 (d, *J* = 6.6 Hz, 3H, H-9′), 0.90 (s, 3H, H-11′), 0.96 (s, 3H, H-10′), 1.08 (s, 3H, H-12′), 1.13 (td, *J* = 3.8, 3.8, 13.2 Hz, 1H, H-8′), 1.29 (m, 1H, H-7″), 1.56 (overlapped, 2H, H-4‴), 1.56 (overlapped, 1H, H-7″), 1.56 (overlapped, 2H, H-4′), 1.56 (overlapped, 1H, H-3′), 1.63 (m, 1H, H-3′), 1.69 (td, *J* = 4.1 Hz, 13.5, 13.6, 1H, H-8′), 1.89 (d, *J* = 6.0 Hz, 1H, H-2′), 1.91 (m, 1H, H-3‴), 2.07 (s, 3H, H-14″), 2.16 (m, 1H, H-4a′), 2.16 (m, 1H, H-3″), 2.88 (d, *J* = 17.0 Hz, 1H, H-1), 3.23 (m, 1H, H-1), 3.23 (m, 2H, H-5‴), 4.58 (m, 1H, H-6″), 4.33 (d, *J* = 17.0 Hz, 1H, H-9), 4.71 (d, *J* = 16.9 Hz, 1H, H-9), 4.79 (dd, *J* = 5.1, 10.7 Hz, 1H, H-2″), 6.69 (s, 1H, H-5). ^{13}C NMR (150 MHz, MeOH-d_4) δ 16.0 (CH$_3$, C-9′), 16.3 (CH$_3$, C-12′), 21.6 (CH$_3$, C-14′), 21.9 (CH$_2$, C-4′), 22.3 (CH$_3$, C-10′), 23.3 (CH$_2$, C-7′), 25.8 (CH$_2$, C-8′), 27.1 (CH$_2$, C-4″), 28.4 (CH$_3$, C-11′), 28.9 (CH$_2$, C-3″), 32.3 (CH$_2$, C-3′), 32.8 (CH$_2$, C-1), 37.8 (C, C-5′), 38.1 (CH, C-2′), 41.9 (CH$_2$, C-5″), 42.3 (CH, C-4a′), 43.5 (C, C-8a′), 45.6 (CH$_2$, C-9), 57.5 (CH, C-2″), 79.4 (CH, C-6′), 99.5 (C, C-1′), 102.3 (CH, C-5), 114.5 (C, C-7), 118.6 (C, C-3), 135.2 (C, C-6), 155.3 (C, C-4), 157.4 (C, C-2), 158.6 (C, C-6″), 171.6 (C, C-8), 172.8 (C, C-13′), 177.4 (C, C-1″). HRMS (10 μg/mL): *m/z* 585.3272 (calcd for [C$_{31}$H$_{45}$N$_4$O$_7$]$^+$ 585.3283, Δ*m*: −1.1 ppm), purity > 96%.

Acetoxystachybotryacetate-arginine (13). Pale yellow powder (1.78 mg, 13%), TLC: 0.54 (DCM/MeOH = 30/70). UV λ$_{max}$ (MeCN/H$_2$O): 238, 264, 300 nm. ^{1}H NMR (600 MHz, MeOH-d_4) δ 0.80 (d, *J* = 6.5 Hz, 3H, H-9′), 0.93 (s, 3H, H-11′), 1.06 (s, 3H, H-10′), 1.17 (s, 3H, H-12′), 1.37 (dd, *J* = 4.4, 12.1 Hz, 1H, H-8′), 1.54 (overlapped, 1H, H-3′), 1.54 (overlapped, 1H, H-4′), 1.58 (m, 2H, H-4‴), 1.60 (m, 1H, H-4″), 1.67 (m, 1H, H-3′), 1.86 (overlapped, 1H, H-8′), 1.86 (overlapped, 1H, H-14′), 1.90 (overlapped, 1H, H-3″), 1.92 (m, 1H, H-2′), 2.13 (s, 3H, H-16′), 2.14 (overlapped, 1H, H-4a′), 2.14 (s, 2H, H-5‴), 2.16 (overlapped, 1H, H-3‴), 2.94 (d, *J* = 17.1 Hz, 1H, H-1), 3.24 (d, *J* = 17.3 Hz, 1H, H-1), 4.36 (d, *J* = 17.0 Hz, 1H, H-9), 4.74 (d, *J* = 16.9 Hz, 1H, H-9), 4.80 (dd, *J* = 5.1, 10.7 Hz, 1H, H-2″), 4.94 (d, *J* = 2.3 Hz, 1H, H-6′), 5.23 (ddd, *J* = 12.8, 4.5, 2.6 Hz, 1H, H-7′), 6.73 (s, 1H, H-5). ^{13}C NMR (150 MHz, MeOH-d_4) δ 15.8 (CH$_3$, C-9′), 17.1 (CH$_3$, C-12′), 20.9 (CH$_3$, C-14′), 21.4 (CH$_3$, C-16′), 21.5 (CH$_2$, C-4′), 21.9 (CH$_3$, C-10′), 27.1 (CH$_2$, C-4″), 28.3 (CH$_3$, C-11′), 28.9 (CH$_2$, C-3″), 31.5 (CH$_2$, C-8′), 32.1 (CH$_2$, C-3′), 33.0 (CH$_2$, C-1), 37.7 (CH, C-2′), 39.1 (C, C-5′), 41.8 (CH$_2$, C-5″), 41.9 (CH, C-4a′), 44.8 (C, C-8a′), 45.5 (CH$_2$, C-9), 57.4 (CH, C-2″), 69.6 (CH, C-7′), 78.2 (CH, C-6′), 99.1 (C, C-1′), 102.5 (CH, C-5), 114.5 (C, C-6), 118.3 (C, C-3), 135.4 (C, C-7), 155.3 (C, C-4), 157.1 (C, C-2), 158.6 (C, C-6″), 171.5 (C, C-8), 172.8 (C, C-15′), 177.4 (C, C-1″). HRMS (10 μg/mL): *m/z* 643.3338 (calcd for [C$_{33}$H$_{47}$N$_4$O$_9$]$^+$ 643.3329, Δ*m*: −0.9 ppm), purity > 95%.

Stachybotry-agmatine (14). Pale yellow powder (10.6 mg, 39%), TLC: 0.35 (EtOAc/MeOH, 50/50 (v/v) + 1% AA). UV λ$_{max}$ (MeCN/H$_2$O): 224, 268, 300 nm. ^{1}H NMR (600 MHz, MeOH-d_4) δ 0.73 (d, *J* = 6.5 Hz, 3H, H-9′), 0.89 (s, 3H, H-10′), 0.98 (s, 3H, H-11′), 1.05 (s, 3H, H-12′), 1.08 (dt, *J* = 3.7, 12.9 Hz, 1H, H-8′), 1.56 (m, 1H, H-7′), 1.56 (overlapped, 2H, H-4′), 1.56 (overlapped, 2H, H-3′), 1.56 (m, 2H, H-3″), 1.76 (m, 2H, H-2‴), 1.84 (m, 1H, H-2″), 1.84 (m, 1H, H-8′), 1.97 (m, 1H, H-7′), 2,11 (dd, *J* = 3.1, 12.2 Hz, 1H, H-4a′), 2.86 (d, *J* = 16,9 Hz, 1H, H-1),3.23 (dd, *J* = 7.8, 14.8 Hz, 1H, H-1), 3.23 (overlapped, 2H, H-4‴), 3.35 (t, *J* =2.9 Hz, 1H, H-6″), 3.60 (dt, *J* = 6.8 Hz, 13.8 Hz, 1H, H-1″), 3.68 (dt, *J* = 7.0, 13.9 Hz, 1H, H-1″), 4.33 (d, *J* = 17.2 Hz, 1H, H-9), 4.51 (d, *J* = 17.2 Hz, 1H, H-9), 6.67 (s, 1H, H-5). ^{13}C NMR (150 MHz, MeOH-d_4) δ 16.0 (CH$_3$, C-9′), 16.5 (CH$_3$, C-12′), 22.1 (CH$_2$, C-4′), 23.0 (CH$_3$, C-10′), 25.4 (CH$_2$, C-8′), 26.0 (CH$_2$, C-7′), 26.5 (CH, C-2″), 27.0 (CH$_2$, C-3′), 29.0 (CH$_3$, C-11′), 32.3 (CH$_2$, C-3′), 33.0 (CH$_2$, C-1), 38.4 (CH, C-2′), 38.7 (C, C-5′), 41.4 (CH, C-4a′), 42.0 (CH$_2$, C-4″), 42.8 (C, C-1″), 43.5 (C, C-8a′), 48.4 (CH$_2$, C-9), 76.4 (CH, C-6′), 99.8 (C, C-1′), 102.1 (CH, C-5), 114.1 (C, C-7), 118.9 (C, C-3), 134.9 (C, C-6), 155.3 (C, C-4), 157.6 (C, C-2), 158.7 (C, C-5″), 171.3 (C, C-8). HRMS (10 μg/mL): *m/z* 499.3279 (calcd for [C$_{28}$H$_{43}$N$_4$O$_4$]$^+$ 499.3268, Δ*m*: −1.1 ppm), purity > 98%.

Stachybotryacetate-agmatine (15). Pale yellow powder (7.2 mg, 22%), TLC: 0.41 (EtOAc/MeOH, 50/50 (v/v) + 1% AA). UV λ$_{max}$ (MeCN/H$_2$O): 224, 268, 300 nm. ^{1}H NMR (600 MHz, DMSO-d_6) δ 0.68 (s, 3H, H-9′), 0.84 (s, 3H, H-11′), 0.89 (s, 3H, H-10′), 0.98 (s, 3H, H-12′), 1.04 (m, 1H, H-8′), 1.52 (overlapped, 1H, H-8′), 1.52 (overlapped, 2H, H-4′), 1.52 (overlapped, 2H, H-3′), 1.52 (overlapped, 2H, H-2″), 1.52 (overlapped, 2H, H-3‴), 1.52 (overlapped, 1H, H-7″), 1.84 (m, *J* = 6.0 Hz, 1H, H-2′), 1.84 (m, 1H, H-7′), 1.99 (s, 3H, H-14′), 2.02 (dd, *J* =3.2, 12.1 Hz, 1H, H-4a′), 2.80 (d, *J* = 17.0 Hz, 1H, H-1), 3.06 (m, 2H, H-4‴), 3.10 (d, *J* =16.9, 1H, H-1), 3.47 (qd, *J* = 6.9, 13.6, 13.7 Hz, 2H, H-1‴), 4.14 (d, *J* =

16.7 Hz, 1H, H-9), 4.39 (d, J = 16.9 Hz, 1H, H-9), 4.49 (t, J = 2.9 Hz, 1H, H-6′), 6.57 (s, 1H, H-5). ^{13}C NMR (150 MHz, DMSO-d_6) δ 15.3 (CH$_3$, C-9′), 15.4 (CH$_3$, C-12′), 20.1 (CH$_2$, C-4′), 20.8 (CH$_3$, C-14′), 21.5 (CH$_3$, C-10′), 21.8 (CH$_2$, C-7′), 24.2 (CH$_2$, C-8′), 24.8 (CH, C-2″), 25.8 (CH$_2$, C-3″), 27.6 (CH$_3$, C-11′), 30.5 (CH$_2$, C-3′), 31.4 (CH$_2$, C-1), 36.0 (CH, C-2′), 36.2 (C, C-5′), 40.1 (CH$_2$, C-4″), 40.3 (CH, C-4a′), 41.1 (C, C-1″), 41.6 (C, C-8a′), 46.5 (CH$_2$, C-9), 76.9 (CH, C-6′), 97.5 (C, C-1′), 100.8 (CH, C-5), 111.7 (C, C-7), 116.2 (C, C-3), 134.0 (C, C-6), 153.8 (C, C-4), 155.6 (C, C-2), 157.0 (C, C-5″), 167.4 (C, C-8), 169.7 (C, C-13′), HRMS (10 μg/mL): m/z 541.3384 (calcd for $[C_{30}H_{45}N_4O_5]^+$ 541.3375, Δm: −1.0 ppm), purity > 96%.

Acetoxystachybotryacetate-agmatine (**16**). Pale yellow powder (5.90 mg, 33%), TLC: 0.40 (EtOAc/MeOH, 50/50 (v/v) + 1% AA). UV λ_{max} (MeCN/H$_2$O): 224, 264, 300 nm. ^{1}H NMR (600 MHz, MeOH-d_4) δ 0.78 (d, J = 6.5 Hz, 3H, H-9′), 0.93 (s, 3H, H-11′), 1.06 (s, 3H, H-10′), 1.16 (s, 3H, H-12′), 1.40 (dd, J = 4.1, 12.6 Hz, 1H, H-8′), 1.53 (overlapped, 1H, H-4′), 1.52 (overlapped, 1H, H-3′), 1.61 (overlapped, 1H, H-4′), 1.61 (overlapped, 2H, H-3‴), 1.67 (ddd, J = 2.6, 4.7, 9.0 Hz, 1H, H-3″), 1.75 (m, 2H, H-2‴),1.82 (d, J = 12.3, 1H, H-8″), 1.86 (s, 3H, H-14′), 1.92 (ddd, J = 4.8, 6.6, 11.6 Hz, 1H, H-2′), 2.09 (s, 3H, H-16′), 2.12 (dd, J =3.1, 12.2 Hz, 1H, H-4a′), 2.93 (d, J = 17.0 Hz, 1H, H-1), 3.24 (overlapped, 2H, H-4‴), 3.24 (overlapped, 1H, H-1), 3.62 (dt, J = 6.9, 6.9, 13.9 Hz, 1H, H-1‴), 3.69 (dt, J = 7.0, 7.0, 14.1 Hz, 1H, H-1″), 4.29 (d, J = 17.0 Hz, 1H, H-9), 4.45 (d, J = 17.0 Hz, 1H, H-9), 4.95 (dd, J = 1.8 Hz, 1H, H-6′), 5.24 (ddd, J = 2.6, 4.6, 12.8 Hz, 1H, H-7′), 6.71 (s, 1H, H-5). ^{13}C NMR (150 MHz, MeOH-d_4) δ 15.8 (CH$_3$, C-9′), 17.2 (CH$_3$, C-12′), 20.9 (CH$_3$, C-14′), 20.9 (CH$_3$, C-16′), 21.5 (CH$_2$, C-4′), 22.0 (CH$_3$, C-10′), 26.5 (CH$_2$, C-2″), 27.0 (CH$_2$, C-3″), 28.3 (CH$_3$, C-11′), 31.5 (CH$_2$, C-8′), 32.1 (CH$_2$, C-3′), 33.0 (CH$_2$, C-1), 37.8 (CH, C-2′), 39.1 (C, C-5′), 42.0 (CH, C-4a′), 42.0 (CH$_2$, C-4″), 42.9 (C, C-1″), 44.8 (C, C-8a′), 48.5 (CH$_2$, C-9), 69.6 (CH, C-7′), 78.4 (CH, C-6′), 99.3 (C, C-1′), 102.6 (CH, C-5), 113.6 (C, C-7), 118.5 (C, C-3), 135.2 (C, C-6), 155.7 (C, C-4), 157.2 (C, C-2), 157.2 (C, C-5″), 171.2 (C, C-8), 172.2 (C, C-13′),172.3 (C, C-15′), HRMS (10 μg/mL): m/z 599.3439 (calcd for $[C_{32}H_{47}N_4O_7]^+$ 599.3428, Δm: −1.1 ppm), purity > 98%.

Microscale Semisynthesis. To investigate different isoindolinone derivatives within one screening, the semisynthesis described above was transferred to a 96-well plate format. In each case, 1.2 μmol of **3** was dissolved in 90 μL of MeCN and reacted with 2 equiv of the corresponding amines dissolved in 30 μL of water. The reaction was carried out under stirring with microstirring magnets for 4 h at RT in the dark. All reaction solutions and further dilutions were stored at −20 °C prior to analysis and biological testing.

LC-MS/MS Microscale Reaction Monitoring. The chromatographic separation and subsequent MS/MS analysis were achieved with a 1260 LC system (Agilent, Waldbronn, Germany), coupled to a QTRAP 5500 mass spectrometer equipped with a Turbo V Ion Source (SCIEX, Darmstadt, Germany). Data acquisition and subsequent data analysis were performed with Analyst 1.6.2. software (SCIEX, Darmstadt, Germany). The gradient started with 10% MeCN + 0.1% FA (solvent **A**) and 95% H$_2$O + 0.1% FA (solvent **B**) for 0.5 min and a flow rate of 0.35 mL/min at a 40 °C column oven temperature. Within 6 min, **A** was increased linearly to 97.5%. For the next 2 min, **A** was held at 97.5%. Equilibration was

performed for 2 min. The source voltage was set to 4.5 kV. The source temperature was set to 500 °C; the curtain gas flow was set to 35 psi, the nebulizer gas was set to 35 psi, and the heater gas was set to 45 psi. Declustering potential (DP) and collision energy voltage (CE) were optimized along with the analyte-specific transitions and measurement modi and are given in Table 2. All LC-MS/MS experiments were performed in unit resolution.

Table 2. MS/MS Parameters for the Monitoring of the Microscale Semisyntheses in the Screening^a

experiment	DP [V]	m/z Q1	m/z Q3	CE [V]	Dwell time [ms]
SRM (QN)	60	487.4	179.0	35	50
SRM (QL1)	60	487.4	119.0	33	50
SRM (QL2)	60	487.4	187.1	27	50
PIS 1	60	350.0−720.0	396.0	60	160
PIS 2	60	400.0−720.0	438.0	45	160
PIS 3	60	350.0−720.0	384.0	60	185

^{a}DP, declustering potential; Q, quadrupole; CE, collision energy; SRM, selected reaction monitoring; QL, qualifier; QN, quantifier; PIS, precursor ion scans.

The microscale reaction solutions were diluted 1/4000 to quantitate the unreacted **3** by SRM experiments and external calibration. For qualitative detection of the formation of the target compounds, precursor ion scans were implemented to the LC-MS/MS method based on the known fragmentation pattern of **3** and **13**. For linear regression, 13 calibration solutions in a concentration range of 0.001−1 μM of a neat standard solution of **3** (10 mg/mL MeCN) were prepared. Quantitation refers to multiple injections of the calibration solutions before and after sample measurement. For further characterization of other side products, all reactions were additionally analyzed by LC-UV-HRMS.

DFT Calculations. The structure of **10** as derived from ^{13}C NMR measurements (Table 1) and the hydride transfer reaction (Figure 5) was also studied by quantum chemical DFT calculations (Table 1) using the TPSS functional, the def2tzvp basis set, and the Grimme dispersion correction GD3BJ, employing the GAUSSIAN G16 package of programs for the gas phase and for the PCM (polarizable continuum model) solvent spheres of water and of MeCN. The results obtained are given in Figure 5. All energies reported refer to ΔG(298 K) [kcal/mol].[31−36]

Serine Protease Inhibition Assay. The inhibitory activity of isolated and semisynthesized compounds toward the coagulation factor XIIa, thrombin, FXa, and trypsin was measured by quantifying the hydrolysis rate of the fluorogenic substrates, as reported previously.[42,47] Briefly, the activity was tested in buffer (10 mM tris−Cl, 150 mM NaCl, 10 mM MgCl$_2$·6H$_2$O, 1 mM CaCl$_2$·2H$_2$O, 0.1% w/v BSA, 0.01% v/v Triton-X100, pH = 7.4) utilizing clear flat-bottom, black polystyrene 96-well plates. The enzymes (human β-FXIIa, HFXIIAB, >95% purity; Molecular Innovations, 2.5 nM—final concentration; human α-thrombin (active) protein, ABIN2127880, >95% purity; antibodies-online, 0.25 nM—final concentration; human factor Xa, HFXA, >95% purity; Molecular Innovations, 2.5 nM—final concentration; porcine trypsin; Merck, 3.5 nM—final concentration) and the fluorogenic substrates for FXIIa: Boc−Gln−Gly−Arg−AMC (Pepta Nova, 25 μM—final concentration, K_m = 167 μM); for

thrombin: Boc−Val−Pro−Arg−AMC (Pepta Nova, 25 μM—final concentration, K_m = 18 μM); for FXa: Boc−Ile−Glu−Gly−Arg−AMC (Pepta Nova, 25 μM—final concentration); and for trypsin: Z−Gly−Gly−Arg−AMC (Sigma-Aldrich, 25 μM—final concentration) were used. Dabigatran (Dabig.), rivaroxaban (Rivar.), and compound "**39b**"[47] were used as positive controls at 500 nM for thrombin, FXa, and FXIIa, respectively. The fluorogenic substrate solution was added into the wells followed by the addition of test compound solution, and the reaction was triggered by the addition of the enzyme solution (final testing volume—150 μL). In the case of blank (substrate + buffer) and control (substrate + enzyme) wells, DMSO was added instead of the test compounds' solution. The fluorescence intensity was measured with a Microplate Reader Mithras LB 940 (Berthold Technologies, excitation at 355 nm, emission at 460 nm) for a period of 1 h with a read every minute. The reactions were performed at 25 °C. To derive IC_{50} values, endpoint RFU (single fluorescence reading after 1 h) was used.[42,47]

Microscale Reaction Product Screening in Thrombin Inhibition Assay. After the reaction conversion was determined by LC-MS/MS (vide supra), frozen samples of the microscale parallel synthesis were defrosted at room temperature and the remaining solvent was removed under the N_2 stream. Each sample was then diluted with the calculated amount of DMSO to set the reaction product concentration to 10 mmol/L. The resulting equimolar samples (36 formed lactams) were screened at 200 μM in thrombin inhibition assay using the fluorogenic substrate. The results of these measurements (triplicate) were expressed as the % of inhibition at 200 μM for each sample.

In Vitro Plasma Coagulation Assays (aPTT and PT). All measurements were performed using citrated (3.8%) human pooled plasma (Dunn Labortechnik GmbH, Germany) on a semiautomated coagulometer (Thrombotimer-2, Behnk Elektronik, Germany) according to the manufacturer's instructions, as previously reported.[42,47] For aPTT measurement, plasma (100 μL) was placed into the incubation cuvettes of the instrument and incubated for 2 min at 37 °C. Then, the test compound solution (10 μL) or solvent (DMSO, 10 μL) was added with a pipette. After 1 min of incubation, 100 μL of prewarmed (37 °C) aPTT reagent (Convergent Technologies, Germany) was added and incubated for an additional 2 min. The cuvettes were transferred to a measuring position, the coagulation was initiated by the addition of 100 μL of $CaCl_2$ solution (25 mM, prewarmed at 37 °C, Convergent Technologies, Germany), and the clotting time was recorded. For PT assays, plasma (100 μL) was incubated for 2 min at 37 °C. Then, the test compound solution (10 μL) or solvent (DMSO, 10 μL) was added with a pipette. After 3 min of incubation, the cuvettes were transferred to a measuring position, the coagulation was initiated by the addition of 100 μL of PT assay reagent already containing $CaCl_2$ (prewarmed at 37 °C, Convergent Technologies, Germany), and the clotting time was recorded.[42,47]

Cytotoxicity Studies. The cytotoxic effects of the isolated and semisynthesized compounds were evaluated with the resazurin assay, performed analogous to previous studies.[48−50] Human liver carcinoma cells (HepG2, HB-8065) and lung adenocarcinoma cells (A549, CCL-185) were cultivated in accordance with the descriptions of Kalinina et al.[51] The cells were seeded with 25,000 cells/well (HepG2) and 10,000 cells/well (A549) in 96-well plates and incubated for 24 h. After

replacing the medium with a serum-free medium, the cells were incubated for an additional 24 h. The PSDs (**1–3, 11–16**) were applied in a concentration range of 0.1−100 μM. All compounds were dissolved in DMSO. The compounds were incubated for 24 h. After the standard resazurin solution, 10 μL was added to the cells and incubated for 2 h at 37 °C. The reduction of resazurin to resorufin was analyzed by screening the fluorescence at λ = 590 nm with a microplate reader (Infinite M200PRO, Tecan, Männendorf, Switzerland). Cytotoxicity assays were performed with three triplicate from three independent passages ($n \geq 9$) for HepG2 cells and with three triplicate from four independent passages ($n \geq 12$) for A549 cells. After subtraction of cell-free blank values, cellular viability was calculated as test over control (T/C). The data are shown as the mean ± standard deviation (SD). T-2 toxin, which was previously isolated in our group, served as the positive control in a concentration of 10 μM.[52] By analysis of variance (one-way ANOVA) and the Tukey post hoc test (*$p \leq 0.05$, **$p \leq 0.01$, ***$p \leq 0.001$), the concentration-dependent effects were analyzed. By log-linear regression, the half-maximal inhibitory concentration (IC_{50}) levels were calculated. The indicated significance represents the significance level relative to the solvent-treated control group (1% DMSO) calculated with the OriginPro 2016G (64-bit) Sr2 b9.3.2.303 (SF8T5-3089-7901139) (OriginLab Corporation, Northampton, MA).

■ ASSOCIATED CONTENT

ⓢ Supporting Information

The Supporting Information is available free of charge at https://pubs.acs.org/doi/10.1021/acsomega.2c05681.

> Spectroscopic data of compounds **10a** and **10b**; DFT calculations and GAUSSIAN 16 Archive entries; semipreparative HPLC-UV chromatograms and NMR spectra for all isolated and semisynthesized compounds (**1−3**; **11−16**); HPLC-MS/MS chromatogram of compound **3**; gradient profiles of semipreparative HPLC-UV; and detailed screening results for thrombin inhibition by 36 PSD derivatives obtained by microscale semisynthesis (PDF)

■ AUTHOR INFORMATION

Corresponding Author

Svetlana Kalinina − *Institut für Lebensmittelchemie, Westfälische Wilhelms-Universität Münster, 48149 Münster, Germany;* ⓞ orcid.org/0000-0001-7564-8213; Phone: +49251 83 33392; Email: s_kali03@uni-muenster.de

Authors

Katharina Steinert − *Institut für Lebensmittelchemie, Westfälische Wilhelms-Universität Münster, 48149 Münster, Germany*

Nina Berg − *Institut für Lebensmittelchemie, Westfälische Wilhelms-Universität Münster, 48149 Münster, Germany*

Dmitrii V. Kalinin − *Institut für Pharmazeutische und Medizinische Chemie, Westfälische Wilhelms-Universität Münster, 48149 Münster, Germany;* ⓞ orcid.org/0000-0003-2717-5364

Annika Jagels − *The Whitney Laboratory for Marine Bioscience, Department of Chemistry, University of Florida, St. Augustine, Florida 32080, United States*

Ernst-Ulrich Würthwein − *Organisch-Chemisches Institut and Center for Multiscale Theory and Computation (CMTC), Westfälische Wilhelms-Universität Münster, 48149 Münster, Germany*

Hans-Ulrich Humpf − *Institut für Lebensmittelchemie, Westfälische Wilhelms-Universität Münster, 48149 Münster, Germany;* ⊙ orcid.org/0000-0003-3296-3058

Complete contact information is available at:
https://pubs.acs.org/10.1021/acsomega.2c05681

Notes

The authors declare no competing financial interest.

■ ABBREVIATIONS

AMV, avian myeloblastosis virus; aPTT, activated partial thromboplastin time; CE, collision energy; DFT, density functional theory; DP, declustering potential; HCD, higher-collisional dissociation; MCTs, macrocyclic trichothecenes; PCM, polarizable continuum model; PDA, potato dextrose agar; PIS, precursor ion scans; PSDs, phenylspirodrimanes; PT, prothrombin time; QL, qualifier transition; QN, quantifier transition; SD, standard deviation; SMTPs, Stachybotrys microspora triprenyl phenols; SRM, selected reaction monitoring

■ REFERENCES

(1) Nikulin, M.; Pasanen, A. L.; Berg, S.; Hintikka, E. L. Stachybotrys Atra Growth and Toxin Production in Some Building Materials and Fodder under Different Relative Humidities. *Appl. Environ. Microbiol.* **1994**, *60*, 3421−3424.

(2) Andersen, B.; Dosen, I.; Lewinska, A. M.; Nielsen, K. F. Pre-Contamination of New Gypsum Wallboard with Potentially Harmful Fungal Species. *Indoor Air* **2017**, *27*, 6−12.

(3) Jarvis, B. B.; Sorenson, W. G.; Hintikka, E. L.; Nikulin, M.; Zhou, Y.; Jiang, J.; Wang, S.; Hinkley, S.; Etzel, R. A.; Dearborn, D. Study of Toxin Production by Isolates of *Stachybotrys chartarum* and Memnoniella Echinata Isolated during a Study of Pulmonary Hemosiderosis in Infants. *Appl. Environ. Microbiol.* **1998**, *64*, 3620−3625.

(4) Dearborn, D. G.; Yike, I.; Sorenson, W. G.; Miller, M. J.; Etzel, R. A. Overview of Investigations into Pulmonary Hemorrhage among Infants in Cleveland, Ohio. *Environ. Health Perspect.* **1999**, *107*, 495−499.

(5) Jagels, A.; Lindemann, V.; Ulrich, S.; Gottschalk, C.; Cramer, B.; Hübner, F.; Gareis, M.; Humpf, H. U. Exploring Secondary Metabolite Profiles of Stachybotrys Spp. By LC-MS/MS. *Toxins* **2019**, *11*, No. 133.

(6) Ekruth, J.; Gottschalk, C.; Ulrich, S.; Gareis, M.; Schwaiger, K. Differentiation of S. Chartarum (Ehrenb.) S. Hughes Chemotypes A and S via FT-IR Spectroscopy. *Mycopathologia* **2020**, *185*, 993−1004.

(7) Jarvis, B. B. *Stachybotrys chartarum*: A Fungus for Our Time. *Phytochemistry* **2003**, *64*, 53−60.

(8) Piontek, M.; Łuszczy, K. Testing the Toxicity of *Stachybotrys chartarum* in Indoor Environments — A Case Study. *Energies* **2021**, *14*, No. 1602.

(9) Hinkley, S. F.; Jiang, J.; Mazzola, E. P.; Jarvis, B. B. Atranones: Novel Diterpenoids from the Toxigenic Mold Stachybotrys Atra. *Tetrahedron Lett.* **1999**, *40*, 2725−2728.

(10) Li, C.; Matsuda, Y.; Gao, H.; Hu, D.; Yao, X. S.; Abe, I. Biosynthesis of LL-Z1272β: Discovery of a New Member of NRPS-like Enzymes for Aryl-Aldehyde Formation. *ChemBioChem* **2016**, *17*, 904−907.

(11) Hasumi, K.; Suzuki, E. Impact of SMTP Targeting Plasminogen and Soluble Epoxide Hydrolase on Thrombolysis, Inflammation, and Ischemic Stroke. *Int. J. Mol. Sci.* **2021**, *22*, No. 954.

(12) Geris, R.; Simpson, T. J. Meroterpenoids Produced by Fungi. *Nat. Prod. Rep.* **2009**, *26*, 1063−1094.

(13) Zhang, P.; Li, Y.; Jia, C.; Lang, J.; Niaz, S.-I.; Li, J.; Yuan, J.; Yu, J.; Chen, S.; Liu, L. Antiviral and Anti-Inflammatory Meroterpenoids: Stachybonoids A−F from the Crinoid-Derived Fungus *Stachybotrys chartarum* 952. *RSC Adv.* **2017**, *7*, 49910−49916.

(14) Jiang, M.; Wu, Z.; Liu, L.; Chen, S. The Chemistry and Biology of Fungal Meroterpenoids (2009−2019). *Org. Biomol. Chem.* **2021**, *19*, 1644−1704.

(15) Jagels, A.; Hövelmann, Y.; Zielinski, A.; Esselen, M.; Köhler, J.; Hübner, F.; Humpf, H.-U. Stachybotrychromenes A−C: Novel Cytotoxic Meroterpenoids from Stachybotrys Sp. *Mycotoxin Res.* **2018**, *34*, 179−185.

(16) Nishimura, Y.; Suzuki, E.; Hasegawa, K.; Nishimura, N.; Kitano, Y.; Hasumi, K. Pre-SMTP, a Key Precursor for the Biosynthesis of the SMTP Plasminogen Modulators. *J. Antibiot.* **2012**, *65*, 483−485.

(17) Yin, Y.; Fu, Q.; Wu, W.; Cai, M.; Zhou, X.; Zhang, Y. Producing Novel Fibrinolytic Isoindolinone Derivatives in Marine Fungus Stachybotrys Longispora FG216 by the Rational Supply of Amino Compounds According to Its Biosynthesis Pathway. *Mar. Drugs* **2017**, *15*, No. 214.

(18) Ayer, W. A.; Miao, S. Secondary Metabolites of the Aspen Fungus Stachybotrys Cylindrospora. *Can. J. Chem.* **1993**, *71*, 487−493.

(19) Hasegawa, K.; Koide, H.; Hu, W.; Nishimura, N.; Narasaki, R.; Kitano, Y.; Hasumi, K. Structure-Activity Relationships of 11 New Congeners of the SMTP Plasminogen Modulator. *J. Antibiot.* **2010**, *63*, 589−593.

(20) Hu, W.; Narasaki, R.; Ohyama, S.; Hasumi, K. Selective Production of Staplabin and SMTPs in Cultures of *Stachybotrys microspora* Fed with Precursor Amines. *J. Antibiot.* **2001**, *54*, 962−966.

(21) Jarvis, B. B.; Salemme, J.; Morais, A. Stachybotys Toxins. 1. *Nat. Toxins* **1995**, *3*, 10−16.

(22) Miyazaki, W.; Kaise, H.; Shinohara, M.; Miyazaki, W.; Izawa, T.; Nakano, Y.; Sugawara, M.; Sugiura, K.; Sasaki, K.; Kaise, H.; Shinohara, M.; Miyazaki, W.; Izawa, T.; Nakano, Y.; Sugawara, M.; Sugiura, K.; Sasaki, K. Structure of K-76, a Complement Inhibitor Produced by Stachybotrys Complementi Nov. Sp. K-76. *J. Chem. Soc. Chem. Commun.* **1979**, *359*, No. 726.

(23) Kaufman, T. S.; Srivastava, R. P.; Sindelar, R. D.; Scesney, S. M.; Marsh, H. C. The Design, Synthesis and Evaluation of A,C,D-Ring Analogs of the Fungal Metabolite K-76 as Complement Inhibitors: A Potential Probe for the Absolute Stereochemistry at Position 2. *Bioorg. Med. Chem. Lett.* **1995**, *5*, 501−506.

(24) Sasaoka, M.; Wada, Y.; Hasumi, K. Stachybotrydial Selectively Enhances Fibrin Binding and Activation of Glu-Plasminogen. *J. Antibiot.* **2007**, *60*, 674−681.

(25) Hasumi, K.; Yamamichi, S.; Harada, T. Small-Molecule Modulators of Zymogen Activation in the Fibrinolytic and Coagulation Systems. *FEBS J.* **2010**, *277*, 3675−3687.

(26) Kaneto, R.; Dobashi, K.; Kojima, I.; Sakai, K.; Shibamoto, N.; YOSHIOKA, T.; Nishida, H.; Okamoto, R.; Akagawa, H.; Mizuno, S. Mer-NF5003B, E and F, Novel Sesquiterpenoids as Avian Myeloblastosis Virus Protease Inhibitors Produced by Stachybotrys Sp. *J. Antibiot.* **1994**, *47*, 727−730.

(27) Roggo, B. E.; Petersen, F.; Sills, M.; Roesel, J. L.; Moerker, T.; Peter, H. H. Novel Spirodihydrobenzofuranlactams as Antagonists of Endothelin and as Inhibitors of HIV-1 Protease Produced by Stachybotrys Sp. I. Fermentation, Isolation and Biological Activity. *J. Antibiot.* **1996**, *49*, 13−19.

(28) Zhao, J. J.; Feng, J.; Tan, Z.; Liu, J.; Zhao, J. J.; Chen, R.; Xie, K.; Zhang, D.; Li, Y.; Yu, L.; Chen, X.; Dai, J. Stachybotrysins A−G, Phenylspirodrimane Derivatives from the Fungus *Stachybotrys chartarum*. *J. Nat. Prod.* **2017**, *80*, 1819−1826.

(29) McDonald, R. S.; Sibley, C. E. The Intramolecular Cannizzaro Reaction of Phthalaldehyde. *Can. J. Chem.* **1981**, *59*, 1061−1067.

(30) Bowden, K.; El-Kaissi, F. A.; Ranson, R. J. Intramolecular Catalysis. Part 5. The Intramolecular Cannizzaro Reaction of o-Phthalaldehyde and [α,A′- 2 H 2]-o-Phthalaldehyde. *J. Chem. Soc., Perkin Trans. 2* **1990**, 2089−2092.

(31) Tao, J.; Perdew, J. P.; Staroverov, V. N.; Scuseria, G. E. Climbing the Density Functional Ladder: Nonempirical Meta−Generalized Gradient Approximation Designed for Molecules and Solids. *Phys. Rev. Lett.* **2003**, *91*, No. 146401.

(32) Grimme, S.; Hansen, A.; Brandenburg, J. G.; Bannwarth, C. Dispersion-Corrected Mean-Field Electronic Structure Methods. *Chem. Rev.* **2016**, *116*, 5105−5154.

(33) Grimme, S.; Ehrlich, S.; Goerigk, L. Effect of the Damping Function in Dispersion Corrected Density Functional Theory. *J. Comput. Chem.* **2011**, *32*, 1456−1465.

(34) Weigend, F.; Ahlrichs, R. Balanced Basis Sets of Split Valence, Triple Zeta Valence and Quadruple Zeta Valence Quality for H to Rn: Design and Assessment of Accuracy. *Phys. Chem. Chem. Phys.* **2005**, *7*, 3297.

(35) Tomasi, J.; Mennucci, B.; Cammi, R. Quantum Mechanical Continuum Solvation Models. *Chem. Rev.* **2005**, *105*, 2999−3094.

(36) Frisch, M. J.; Trucks, G. W.; Schlegel, H. B.; Scuseria, G. E.; Robb, M. A.; Cheeseman, J. R.; Scalmani, G.; Barone, V.; Petersson, G. A.; Nakatsuji, H.; Li, X.; Caricato, M.; Marenich, A. V.; Bloino, J.; Janesko, B. G.; Gomperts, R.; Mennucci, B.; Hratch, D. J. *Gaussian 16*, revision B.01; Gaussian, Inc.: Wallingford CT, 2016.

(37) Fredenhagen, H.; Bonhoeffer, K. F. Untersuchungen Über Die CANNIZZAROsche Reaktion in Schwerem Wasser. *Z. Phys. Chem.* **1937**, *181A*, 379−391.

(38) Augner, D.; Gerbino, D. C.; Slavov, N.; Neudörfl, J.-M.; Schmalz, H.-G. N -Capping of Primary Amines with 2-Acyl-Benzaldehydes To Give Isoindolinones. *Org. Lett.* **2011**, *13*, 5374−5377.

(39) Matsumoto, N.; Suzuki, E.; Tsujihara, K.; Nishimura, Y.; Hasumi, K. Structure−Activity Relationships of the Plasminogen Modulator SMTP with Respect to the Inhibition of Soluble Epoxide Hydrolase. *J. Antibiot.* **2015**, *68*, 685−690.

(40) Lim, H. A.; Joy, J.; Hill, J.; San Brian Chia, C. Novel Agmatine and Agmatine-like Peptidomimetic Inhibitors of the West Nile Virus NS2B/NS3 Serine Protease. *Eur. J. Med. Chem.* **2011**, *46*, 3130−3134.

(41) Peterlin Masic, L. Arginine Mimetic Structures in Biologically Active Antagonists and Inhibitors. *Curr. Med. Chem.* **2006**, *13*, 3627−3648.

(42) Korff, M.; Imberg, L.; Will, J. M.; Bückreiß, N.; Kalinina, S. A.; Wenzel, B. M.; Kastner, G. A.; Daniliuc, C. G.; Barth, M.; Ovsepyan, R. A.; Butov, K. R.; Humpf, H.-U.; Lehr, M.; Panteleev, M. A.; Poso, A.; Karst, U.; Steinmetzer, T.; Bendas, G.; Kalinin, D. V. Acylated 1H-1,2,4-Triazol-5-Amines Targeting Human Coagulation Factor XIIa and Thrombin: Conventional and Microscale Synthesis, Anticoagulant Properties, and Mechanism of Action. *J. Med. Chem.* **2020**, *63*, 13159−13186.

(43) Harrach, B.; Bata, A.; Sándor, G.; Ványi, A. Isolation of Macrocyclic and Non-Macrocyclic Trichothecenes (Stachybotrys and Fusarium Toxins) from the Environment of 200 III Sport Horses. *Mycotoxin Res.* **1987**, *3*, 65−68.

(44) Harrach, B.; Bata, A.; Bajmocy, E.; Benko, M. Isolation of Satratoxins from the Bedding Straw of a Sheep Flock with Fatal Stachybotryotoxicosis. *Appl. Environ. Microbiol.* **1983**, *45*, 1419−1422.

(45) Drobotko, V.; Drobot'ko, V. G. Stachybotryotoxicosis. A New Disease of Horses and Humans. *Am. Rev. Sov. Med.* **1945**, *2*, 238−242.

(46) Smedsgaard, J. Micro-Scale Extraction Procedure for Standardized Screening of Fungal Metabolite Production in Cultures. *J. Chromatogr. A* **1997**, *760*, 264−270.

(47) Platte, S.; Korff, M.; Imberg, L.; Balicioglu, I.; Erbacher, C.; Will, J. M.; Daniliuc, C. G.; Karst, U.; Kalinin, D. V. Microscale Parallel Synthesis of Acylated Aminotriazoles Enabling the Development of Factor XIIa and Thrombin Inhibitors. *ChemMedChem* **2021**, *16*, 3672−3690.

(48) Mosmann, T. Rapid Colorimetric Assay for Cellular Growth and Survival: Application to Proliferation and Cytotoxicity Assays. *J. Immunol. Methods* **1983**, *65*, 55−63.

(49) Nociari, M. M.; Shalev, A.; Benias, P.; Russo, C. A Novel One-Step, Highly Sensitive Fluorometric Assay to Evaluate Cell-Mediated Cytotoxicity. *J. Immunol. Methods* **1998**, *213*, 157−167.

(50) O'Brien, J.; Wilson, I.; Orton, T.; Pognan, F. Investigation of the Alamar Blue (Resazurin) Fluorescent Dye for the Assessment of Mammalian Cell Cytotoxicity. *Eur. J. Biochem.* **2000**, *267*, 5421−5426.

(51) Kalinina, S. A.; Jagels, A.; Hickert, S.; Mauriz Marques, L. M.; Cramer, B.; Humpf, H.-U. U. Detection of the Cytotoxic Penitrems A−F in Cheese from the European Single Market by HPLC-MS/MS. *J. Agric. Food Chem.* **2018**, *66*, 1264−1269.

(52) Beyer, M.; Ferse, I.; Humpf, H.-U. Large-Scale Production of Selected Type A Trichothecenes: The Use of HT-2 Toxin and T-2 Triol as Precursors for the Synthesis of d 3-T-2 and d 3-HT-2 Toxin. *Mycotoxin Res.* **2009**, *25*, 41−52.